Hypoxia Regulates Lymphoid Development of Human Hematopoietic Progenitors

Sara Chabi, Benjamin Uzan, Irina Naguibneva, Julien Rucci, Lucine Fahy, Julien Calvo, Marie-Laure Arcangeli, Frédéric Mazurier, Françoise Pflumio, Rima Haddad

Hypoxia regulates lymphoid development of human hematopoietic progenitors

Sara Chabi[1-4], Benjamin Uzan[1-4], Irina Naguibneva[1-4], Julien Rucci[1-4], Lucine Fahy[1-4], Julien Calvo[1-4], Marie-Laure Arcangeli[1-4], Frédéric Mazurier[5,6], Françoise Pflumio[1-4†] and Rima Haddad[1-4†*§]

1. UMR Stabilité Génétique Cellules Souches et Radiations, Université de Paris, CEA, 18 route du Panorama, 92260 Fontenay-aux-Roses, France ;

2. UMR Stabilité Génétique Cellules Souches et Radiations, Université Paris Sud, Université Paris-Saclay, CEA, 18 route du Panorama, 92260 Fontenay-aux-Roses, France ;

3. Team Niche and Cancer in Hematopoiesis, U1274, Inserm, 18 route du Panorama, 92260 Fontenay-aux-Roses, France ;

4. Laboratory of Hematopoietic Stem Cells and Leukemia/Service Stem Cells and Radiation /iRCM/JACOB/DRF, CEA, 18 route du Panorama, 92260 Fontenay-aux-Roses, France ;

5. Université de Tours, EA7501 GICC, Tours, France ;

6. CNRS ERL7001 LNOx, Tours, France ;

†co-authorship

*Corresponding author: Dr. Rima Haddad, PhD. https://orcid.org/0000-0001-7040-843X

§Lead Contact : Rima Haddad

E-mail: rima.haddad@u-psud.fr; rima.haddad@universite-paris-saclay.fr

Abstract

Hypoxia plays major roles in the physiology of hematopoietic and immune niches. Important clues from works in mouse have paved the way to investigate the role of low O_2 levels in hematopoiesis. However whether hypoxia impacts the initial steps of human lymphopoiesis remained unexplored. Here, we show that hypoxia regulates cellular and metabolic profiles of umbilical cord blood (UCB)-derived hematopoietic progenitor cells. Hypoxia more specifically enhances *in vitro* lymphoid differentiation potentials of lymphoid-primed multipotent progenitors (LMPPs) and Pro-T/NK cells and *in vivo* B cell potential of LMPPs. In accordance, hypoxia exacerbates the lymphoid gene expression profile through HIF-1α (for LMPPs) and HIF-2α (for Pro-T/NK). Moreover, loss of HIF-1/2α expression seriously impedes NK and B cell production from LMPPs and Pro-T/NK. Our study thus describes how hypoxia contributes to the lymphoid development of human progenitors and reveals the implication of the HIF pathway in LMPPs and Pro-T/NK-cell lymphoid identities.

Introduction

Adult hematopoiesis proceeds in the bone marrow (BM) microenvironment that is characterized by low oxygen (O_2) partial pressure (pO_2: 1-6% O_2) commonly called hypoxia (Chow et al., 2001; Eliasson and Jonsson, 2010; Kubota et al., 2008; Levesque et al., 2007; Mendelson and Frenette, 2014; Mohyeldin et al., 2010; Morrison and Scadden, 2014; Nombela-Arrieta et al., 2013; Parmar et al., 2007; Semenza, 2012; Simsek et al., 2010; Spencer et al., 2014; Suda et al., 2011). Hypoxia stabilizes the hypoxia-inducible factor-1/2α (HIF-1/2α) proteins, which represent master regulators of hypoxia transcriptional response at the cellular and systemic levels, and activate several downstream effectors of HIF pathway (Imanirad et al., 2014; Majmundar et al., 2010; Rouault-Pierre et al., 2013; Semenza, 2012; Takubo et al., 2010).

So far, functional studies related to the impact of hypoxic niches on hematopoietic progenitor development have been mostly performed in the mouse (Chow et al., 2001; Cipolleschi et al., 1993; Eliasson and Jonsson, 2010; Imanirad et al., 2014; Kubota et al., 2008; Mohyeldin et al., 2010; Morrison and Scadden, 2014; Parmar et al., 2007; Semenza, 2012; Simsek et al., 2010; Suda et al., 2011). In human, hypoxia promotes the formation of myelo-erythroid colonies and enhances maintenance, expansion and proliferative capacities of hematopoietic stem/progenitor cells (HSPCs) tested *in vitro* and *in vivo* in immune-deficient mouse models (Cipolleschi et al., 1997; Danet et al., 2003; Guitart et al., 2010; Hammoud et al., 2012; Ivanovic et al., 2000; Ivanovic et al., 2004; Koller et al., 1992; Rouault-Pierre et al., 2013; Shima et al., 2009). Furthermore usage of cyclosporin A on mouse BM and umbilical cord blood (UCB) HSPCs, mimicking artificial hypoxic atmosphere, protected transplantable HSPCs from ROS-dependent loss of function (Mantel et al., 2015). However, even though hypoxia maintains a variety of early hematopoietic precursors in mouse and human, the understanding of HIF factor role in hematopoiesis have been mostly addressed in the mouse focusing on hematopoietic stem cell (HSC) functions (Guitart et al., 2013; Halvarsson et al., 2017; Krock et al., 2015; Takubo et al., 2010; Vukovic et al., 2016). An initial study by the group of T. Suda, based on a conditional *Hif-1α* knockout strategy, underlines progressive exhaustion of HSCs upon serial transplantation, concluding that Hif-1α is essential for HSC maintenance (Takubo et al., 2010). Using constitutive or inducible hematopoiesis-specific Hif deletion, works by the group of K.R. Kranc showed that Hif-1α or Hif-2α ablation did not affect HSC survival/numbers, self-renewal capacity, multipotency upon serial transplantation and recovery after hematopoietic injury providing evidence that Hif-1α and Hif-2α are dispensable for cell autonomous HSC maintenance (Guitart et al., 2013; Vukovic et al., 2016). Recently, the work by Halvarsson *et al.* (Halvarsson et al., 2017) showed that genetic ablation of Hif-1α did not affect engraftment of both HSCs and multipotent progenitors upon transplantation to recipient mice which almost relied, in condition of

oxygen deprivation, on pyruvate dehydrogenase kinase 1 (Pdk1) a robust hypoxia-inducible gene mediated by Hif-1α, suggesting no links between Pdk1 and Hif-1α (Halvarsson et al., 2017). Finally the work by Krock et *al*., relying on the deletion, in the hematopoietic system, of the aryl hydrocarbon receptor nuclear translocator (ARNT), the Hif-1α and Hif-2α dimerization partner, indicates that both Hif-1α and Hif-2α are required for adult and fetal HSC viability and homeostasis (Krock et al., 2015).

In humans, the work by Rouault *et al*. emphasizes the role of HIF-2α, and to a lesser extent HIF-1α, in the maintenance and viability of early $CD34^{+}CD38^{+/-}$ HSPCs but whether HIF factors are involved in the function of human early lymphoid progenitors remained elusive (Rouault-Pierre et al., 2013).

Immune cells are also subjected to different levels of O_2 depending on their home-tissue (Hale et al., 2002; McNamee et al., 2013; Ohta et al., 2011). While B cells are exposed to low O_2 levels within spleen and lymph nodes, NK-cells preferentially locate in the most hypoxic area, whereas NKT-cells and T-cells are less sensitive to hypoxic O_2 levels (Ohta et al., 2011). The thymus is more hypoxic than the spleen and lymph nodes with scattered hypoxic regions observed in the cortex and medulla, probably due to a blood microvasculature (Hale et al., 2002). These observations suggest that the variation in the degree of oxygenation among lymphoid organs and cell types (Ohta et al., 2011) plays a physiologic role. Indeed, hypoxia/HIF pathway has been described as a regulator of immune functions. In mouse, cytotoxic T lymphocytes develop more efficiently and are more lytic in hypoxic than in normoxic atmospheres (Caldwell et al., 2001). Hypoxia is also able to drive an anti-inflammatory program enabling an increase of $CD4^{+}CD25^{+}$ regulatory T lymphocyte numbers and suppressive properties (Ben-Shoshan et al., 2008). In human, hypoxia can improve proliferation, viability and cytotoxicity of effector memory T-cells but decreases these parameters from naive and central memory T-cells (Xu et al., 2016), and also affects NK cell differentiation *in vitro* (Yun et al., 2011). Furthermore, HIF pathway plays a prominent role in regulating antitumor activity in cytotoxic T lymphocytes (Palazon et al., 2017) and vital functions of B lymphocytes in germinal centers (Cho et al., 2016). Deletion of HIF-1α in NK cells was shown to inhibit tumor growth by stimulating non-productive angiogenesis and despite impaired tumor cell killing (Krzywinska et al., 2017). However the actual contribution of low O_2 levels to human hematopoietic progenitor cells (HPCs) with lymphoid fate and potentials remains an elusive issue.

The early steps of human lymphopoiesis in the fetus and in the adult comprise several intermediate cell populations that pave the multiple steps of T-, B- and NK-cell development. Over the past few decades, a revised map of the phyletic relationships between early lympho-myeloid progenitors have been proposed with distinct subpopulations of $CD34^{+}CD45RA^{+}$ HPCs being identified as multilymphoid progenitors (Alhaj Hussen et al., 2017; Belluschi et al., 2018; Blom and Spits, 2006; Doulatov et al., 2010; Doulatov et al., 2012; Galy et al., 1995; Goardon et al., 2011; Haddad et al., 2004;

Haddad et al., 2006; Hao et al., 1998; Karamitros et al., 2018; Kohn et al., 2012; Notta et al., 2016; Six et al., 2007). Particularly, early lymphoid progenitors (ELPs) were characterized by their substantial capacity to give rise to T-, B- and NK-cells while conserving some myeloid (*i.e* dendritic and monocytic) differentiation abilities. ELPs were especially selected on the basis of cell surface markers that traditionally identify early T/NK or B lymphoid developmental pathway such as CD7 and/or CD10 and on the presence or not of CD38 (Doulatov et al., 2010; Galy et al., 1995; Haddad et al., 2004; Hao et al., 1998; Six et al., 2007). Upstream of the ELP, several groups recently described a lymphoid-primed multipotent progenitor (LMPP) cell population capable to develop into lymphoid cells, and still having granulocytes and/or monocytes and dendritic cell potentials, expressing or not CD38 but lacking cell surface expression of typical lymphoid markers (Goardon et al., 2011; Karamitros et al., 2018; Kohn et al., 2012). These cell populations, that are located in the BM, participate in the production of lymphoid cells during life time.

Interestingly studies regarding human lymphoid development/differentiation, that mostly rely on *in vitro* assays, have always been conducted in 21% O_2 (normoxic/hyperoxic conditions) somehow in contradiction with the low *in vivo* O_2 concentrations of the BM or of the thymus. Conventional *in vitro* cell culture conditions thus appear not suitable for the proper exploration of human lymphopoiesis since they do not accurately reproduce the physiologic O_2 tissue levels.

In the present study we evaluated how important are low O_2 levels in maintaining and engaging phenotypically distinct human HPCs polarized towards the lymphoid lineage. We show that low O_2 differentially affect HPC populations and specifically enhance lymphoid development from LMPPs and Pro-T/NK uncovering an unsuspected implication of hypoxia and HIF pathway in human early lymphopoiesis.

Results

Hypoxia impacts cellular and metabolic profile of UCB-derived hemato-lymphoid progenitors

Direct *in vivo* measurements of local pO_2 in the BM of live mice showed that peri-sinusoidal regions of large blood vessels located far from the endosteal surface, and which contain HSCs, exhibit very low O_2 levels (pO_2: 1.3%) whereas sites located at the close vicinity of the osteoblastic niche, supposedly occupied by lymphoid progenitors, are less hypoxic with a pO_2 around 3% (Ding and Morrison, 2013; Spencer et al., 2014). Furthermore works on human total UCB-derived $CD34^+$ cells indicated that a concentration of 3% O_2 allowed HIF-1α and HIF-2α target gene expression (Rouault-Pierre et al., 2013), and that frequency of

Scid Repopulating Cells at day-0 and at day-10 in co-cultures at 5% and 1.5% O_2 were similar (Hammoud et al., 2012). Thus, 3.5% of O_2 levels were chosen in our experiments to mimic physiologic hypoxic atmosphere potentially favorable for maintenance of human HPCs endowed with a lymphoid potential. To assess the consequences of a hypoxic environment in lymphoid cell development/differentiation, five subpopulations of UCB HPCs, *i.e.* $CD34^+CD38^{lo/-}CD45RA^-CD90^+$ HSPCs, $CD34^+CD38^{lo/-}CD45RA^-CD90^-$ MPPs (Majeti et al., 2007), $CD34^+CD45RA^{hi}CD7/10/19^-CD62L^{hi}(CD38^+/CD38^-)$ LMPPs (Goardon et al., 2011; Karamitros et al., 2018; Kohn et al., 2012), $CD34^+CD45RA^{hi}CD7^+$ ELPs (thereafter called Pro-T/NK) and $CD34^+CD45RA^{hi}CD7/19^-CD10^+$ ELPs (thereafter called Pro-B) (Haddad et al., 2004; Haddad et al., 2006; Haddad et al., 2008; Larbi et al., 2014) (Figure 1A and Figure S1A) were sorted and short-term cultured in contact with the mouse MS-5 stromal cells, that we and others previously showed as being able to support maintenance and growth of human lymphoid progenitors (Berardi et al., 1997; Haddad et al., 2004; Haddad et al., 2008; Larbi et al., 2014; Robin et al., 1999), in low (3.5%) and high (21%) O_2 levels (Figure 1B for protocol, Figures S1Bi, S1Bii and S1C for sorting gates and frequencies). After one week of culture, the percentages of $CD34^+$ cells obtained from HSPCs, MPPs, LMPPs and Pro-T/NK remained significantly higher in low versus high O_2 concentrations (Figure 1C). However, HSPC, MPP and LMPP cultures under low O_2 levels resulted in lower $CD34^+$ absolute cell numbers in comparison with 21% O_2 whereas Pro-T/NK and Pro-B cells produced similar $CD34^+$ cell numbers (Figure 1D). The phenotypes of the various HPC-derived $CD34^+$ cells were similar in terms of CD7, CD19, CD45RA and CD10 expression when comparing low and high O_2 levels and resembled the HPC day-0 original phenotype (Figure S1D) indicating that the culture conditions could maintain the phenotypic profiles of native fresh cells independently of O_2 level.

As apoptosis was similar among HPC-derived $CD34^+$ cells under hypoxia and normoxia in these conditions (Figure 1E), we examined whether hypoxia inhibited growth of HSPCs, MPPs, LMPPs and Pro-T/NK cells. Ki67 staining showed that low O_2 levels reduce HPCs proliferation (Figure 1F) with cell cycle progression being impeded in HSPCs, MPPs, LMPPs and Pro-T/NK-derived $CD34^+$ cells (Figure 1G). Taken together, these results show that low O_2 concentration prevents cell proliferation and induces cell quiescence in HSCs, MPPs, LMPPs and Pro-T/NK-cells, which favors the maintenance of an immature phenotype.

Low-O_2 environment tolerance of HSPCs is essential for their properties and function (Guitart et al., 2010; Mohyeldin et al., 2010; Suda et al., 2011), and requires significant metabolic adaptation (Simsek et al., 2010). We thus investigated whether hypoxia regulates the mitochondrial state of the various HPCs through autophagy potential modification in these different hematopoietic populations. Cyto-ID staining, that allows monitoring the global autophagy process in live cells (Gomez-Puerto et al., 2016), revealed

important basal autophagy of HSPCs, MPPs, LMPPs and Pro-T/NK-derived cells in normoxic and hypoxic conditions nonetheless with a diminution of autophagy-related vesicles, in low compared to high O_2 concentrations (Figure 1H). Flow cytometry measurement of the mitochondrial mass with Mitotracker Green (MTG) and mitochondrial membrane potential with Tetramethylrhodamine ethyl ester (TMRE) revealed that hypoxia favors mitochondrial rest in HSPCs, MPPs and LMPPs (Figure 1I and Figure S1E). Interestingly, MTG fluorescence was slightly enhanced in presence of verapamil in line with recent findings in murine HPCs (de Almeida et al., 2017) but without major changes comparing normoxia and hypoxia conditions (Figure S1F). Taken together these results indicate that low O_2 levels induce cell resting, reduce autophagy and prevent human hemato-lymphoid progenitors from mitochondrial activation which is likely a consequence of cell hypoxia induced-quiescence (Ianniciello et al., 2017; Simsek et al., 2010).

Hypoxia increases *in vitro* lymphoid differentiation of LMPPs and Pro-T/NK cells

HPC-derived cells recovered from high and low O_2 conditions were tested for their lymphoid differentiation potentials using limiting-dilution assays (LDA) and bulk cultures, enabling to functionally characterize the impact of O_2 levels on the generation of NK, B and T lymphoid cells (Figure 1B). NK-cell precursor frequencies were greatly higher among MPP-, LMPP- and Pro-T/NK-derived cells after low O_2 compared to high O_2 cultures and interestingly were close to those obtained from day-0 non-manipulated cells indicating maintenance of NK potential in hypoxia (Figure 2A, Figures S2A and S3A). B-cell precursor frequencies tended to decrease or were similar in hypoxic HSPCs or MPPs cultures compared to normoxic conditions but higher to day-0 cells (Figure 2B and Figure S2A), in line with the results of bulk B-cell cultures (Figure S3B). These enhanced B cell potentials may be related to the lymphoid inductive support of MS-5 stromal cells (Berardi et al., 1997; Haddad et al., 2004). Interestingly LMPP cells behaved differently, with enhanced B cell potentials when LMPP-derived cells were recovered from low compared to high O_2 levels, reaching similar levels to non-manipulated day-0 LMPPs (Figure 2B and Figure S2A). Finally, LMPP- and Pro-T/NK-derived cells were tested for T cell potentials using co-cultures with MS-5 stromal cells expressing the Notch ligand Delta-like1 (MS-5/DLL1) (Calvo et al., 2012). On the basis of total $CD7^+$ cells as well as committed $CD4^+CD3^-CD8^-$ intermediate simple positive (ISP), $CD4^+CD8^+$ double positive (DP) and total $CD3^+$ T cells (see Figure S2B for strategy analysis), we observed that low O_2 levels substantially raised frequencies and production of human T cells from Pro-T/NK cells but not from LMPPs compared to 21% O_2 (Figure 2C and Figure S2A). Yet, in bulk cultures, T-lymphocytes production from LMPPs appeared to be dependent on O_2 levels with a moderate albeit significant increase of $CD7^+CD5^+$ T cell numbers in low O_2 concentrations (Figure S3C) but with T cell

differentiation not significantly different from high O_2 (Figures S3C and S3D). Interestingly, the proportion of wells seeded with 300 Pro-T/NK cells that contained $CD3^+$ T cells was higher in low O_2 condition as well as the percentage of $CD3^+$ cells after hypoxia treatment in comparison to day-0 or normoxia Pro-T/NK counterpart (7.4% ± 2.6% relative to 1.4% ± 0.3% and 3.2% ± 1% respectively) (Figure S2C), as observed in bulk cultures (22.3% ± 11.1% relative to 6.1% ± 1.1% and 9.4% ± 2.3% respectively) (Figure S3D).

Altogether these results indicate that, in comparison to high O_2, low O_2 levels empower NK-cell development from MPPs, LMPPs and Pro-T/NK cells and B- and T- cell generation capacity respectively from LMPPs and Pro-T/NK and preserved the intrinsic lymphoid-cell production capability compared to the day-0 cell counterpart.

Based on the overall functional results, and to dig into the contribution of hypoxia in the early steps of human lymphopoiesis we next focused our study on LMPPs and Pro-T/NK cells as original human lymphoid progenitor cells targeted by hypoxia.

Hypoxia maintains *in vivo* B cell lymphoid potential of LMPPs

Because *in vitro* cultures may not mimic physiologic cell development, we investigated to which extent early lymphoid progenitors submitted to hypoxia retained their differentiation ability *in vivo* using xenograft models, the gold standard assay to follow human blood cell development (Doulatov et al., 2012). As we observed that hypoxia preserves *in vitro* B cell lymphopoiesis of LMPPs (Figure 2B), we tested the potentials of day-0 native LMPPs and low and high O_2 LMPP-derived cells after injection of cells in NSG mice carrying the c-Kit/W41 (NSG-W41) mutation that supports human hematopoiesis without prior myelo-ablation (Cosgun et al., 2014) (Figure 1A for protocol). We used these mouse recipients because transplantation of LMPPs in irradiated NSG mice may result in high myeloid cell development and may complicate B cell lineage analyses ((Kohn et al., 2012; Mazurier et al., 2003) and data not shown). LMPP-derived cells from low O_2 cultures generated similar human hematopoietic recovery than non-manipulated cells but higher engraftment capacity in comparison to normoxic condition (with mean ± SEM: 0.08% ± 0.02% and 0.34% ± 0.11% of $hCD45^+$ cells from normoxic and hypoxic conditions respectively, $p = 0.03$) (Figure 3A). Human hematopoietic cells were mainly B cells yet with no significant difference between low and high O_2 conditions (Figure 3B). Absolute B cell numbers were higher in mice transplanted with LMPPs-derived cells isolated from low compared to high O_2 levels, with 3 times more B cells recovered from LMPPs kept in hypoxia in comparison to normoxia (Figure 3C). It is to be noted that we were unable to detect any T cells in the thymus and spleen of immunodeficient mice

transplanted with LMPP derived cells from hypoxia and normoxia cocultures. Of note we did not perform xenotransplantation of treated Pro-TNK cells because of their low engraftment and homing potential in the post-natal thymus of immunodeficient mice, a major limitation for the testing of their T cell development ability (Haddad et al., 2004).

Taken together with the *in vitro* results, these observations show that hypoxia helps maintaining intrinsic human lymphoid cell potentials, including B cell potential, in LMPPs.

Hypoxia empowers lymphoid molecular identity of LMPPs and Pro-T/NK cells

As lymphoid potential of LMPP and Pro-T/NK cells is highly sensitive to O_2 levels, we first studied how low O_2 differentially impact the expression of genes known to regulate early lymphoid specification and lymphoid potential of LMPP and Pro-T/NK cells compared to normoxia. After a 7-days exposure to low and high O_2 (Figure 1A), we found no differential expression of the early NK cell markers *ID2* (Blom and Spits, 2006) and *TOX2* (Vong et al., 2014), of B cell commitment marker *IKAROS* and of T lymphoid primed progenitor markers *IRF4* and *CCR9* (Wang et al., 2015) (Figures 4A and 4B). On the contrary mRNA levels of *FLT3* and *CEBPA* (Adolfsson et al., 2005), of *SOX4* known to facilitate B and T cell differentiation and of *NOTCH1* and *IL15RA* early T/NK markers (Felices et al., 2014; Laurenti et al., 2013; Schilham et al., 1997; Schilham et al., 1996; Yu et al., 2013) were increased in LMPPs and Pro-T/NK in low O_2. Interestingly, mRNA levels of B cell specification markers *BCL11A* and *E2A* (Blom and Spits, 2006; Chambers et al., 2007; Laurenti et al., 2013; O'Riordan and Grosschedl, 1999) were increased in LMPP cells following low O_2 treatment (Figures 4A) as were mRNA levels of early T/NK cell development-associated genes *IL7RA* and *RAG1* in Pro-T/NK-derived cells after exposure to low O_2 levels (Blom and Spits, 2006; Boos et al., 2008; Yu et al., 2013) (Figure 4B). Overall we observed a "lymphoid-biased" gene signature that correlated with the enhanced LMPP and Pro-T/NK cell potentials in low O_2.

Several reports indicate that HIF-1α factor is dispensable for murine long term hematopoiesis (Guitart et al., 2013; Vukovic et al., 2016) but it favors hematopoiesis from human HSPCs (Rouault-Pierre et al., 2013), indicating controversies between mouse and human analyses. Interestingly HIF-1α implication in the early steps of human lymphopoiesis has not been investigated so far. These different elements led us to study its expression in LMPP- and Pro-T/NK-derived cells recovered from low and high O_2 . *HIF-1A* mRNA levels were similar in cells from both conditions (Figure 4C) but, as expected, HIF-1α protein was stabilized and localized in the nucleus of LMPP- and Pro-T/NK-derived cells only after recovery from low O_2 (Figure 4D). This nuclear translocation was associated with increased mRNA levels of the HIF-1α target genes *VEGFA, CXCR4*, the latter being also expressed during early lymphopoiesis (Aiuti et al.,

1999; Haddad et al., 2006), and/or *GLUT3* (Figure 4E) (Fang et al., 2009; Forristal et al., 2015; Kuang et al., 2017; Rouault-Pierre et al., 2013; Testa et al., 2016).

Taken together, these results indicated that the hypoxia signature correlated with enhanced cellular and molecular lymphoid identities of LMPP and Pro-T/NK-derived cells compared to normoxia.

Silencing of *HIF-1A* and *HIF-2A* affects lymphoid molecular profiles in LMPPs and Pro-T/NK cells

We next studied the role of HIF-1α in sustaining LMPPs and Pro-T/NK cell lymphoid identities using HIF-1α knocked down (KD) with lentiviral vectors encoding a green fluorescent protein (GFP) reporter together with a small hairpin RNA (shRNA) directed against the *HIF-1A* (HIF-1α KD) (Rouault-Pierre et al., 2013) (Figure S4A). Efficient transduction (≥60%, Figure S4B) of LMPP- and Pro-T/NK-derived cells induced a strong reduction of HIF-1α mRNA levels and protein (Figure 5A, and Figures S4C and S4D) in association with *VEGFA* target gene down-regulation during culture at low O_2 levels (Figure 5B). We next measured lymphoid specification gene expression levels following HIF-1α KD, and directly after a period of co-culture under hypoxia, to investigate the putative connection between HIF-1α and lymphoid marker expression of LMPPs and Pro-T/NK cells (Figure S4A). Interestingly, many lymphoid-related genes that were up-regulated in LMPP-derived cells recovered from hypoxia (Figure 4A) were down-regulated in HIF-1α KD cells (Figure 5C, left panel), supporting the idea that HIF-1α participates in the maintenance of lymphoid identity in LMPPs in low O_2 concentrations. In contrast, HIF-1α KD in Pro-T/NK cells did not modify S*OX4*, *BCL11A*, *NOTCH1* expression that remained up-regulated after hypoxia treatment whereas *FLT3*, *RAG1, IL7RA* and *IL15RA* expressions were even further increased (Figure 5C, right panel).

As transduced HIF-1α KD Pro-T/NK cells were kept in hypoxia prior molecular analyses were done, we wondered whether a HIF-1α redundant factor could interfere with lymphoid marker expression in Pro-T/NK cells. We hypothesized that *HIF-2A*, which transcriptional expression was unchanged in HIF-1α KD/LMPP and /Pro-T/NK cells (Figure 5B) may take part in the hypoxia-related lymphoid potential regulation. We thus knocked down HIF-2α in Pro-T/NK cells (Figures S4A, S4B and Figure 5D). *GLUT3* expression was significantly decreased upon *HIF-1A* KD whereas *CXCR4* and HIF-2 α target gene *HES1* expression (Rouault-Pierre et al., 2013) were more sensitive to HIF-2α KD and *VEGFA* levels were almost equally affected by HIF-1/2α KD (Figure 5E). As *CXCR4* was upregulated in Pro-T/NK-derived cells recovered from hypoxia (Figure 4E) and decreased in HIF-2α KD (Figure 5E), it appears that HIF-2α

regulates *CXCR4* expression in hypoxic Pro-T/NK cells. Remarkably, while *HIF-2A* silencing in hypoxic Pro-T/NK cells did not change neither *FLT3* nor *NOTCH1* expression, it significantly decreased mRNA levels of *SOX4*, *BCL11A*, *IL7RA*, *IL15RA* and *RAG1* suggesting a role of HIF-2α in upregulating the lymphoid program of Pro-T/NK cells subjected to low O_2 levels (Figure 5F).

Altogether, these results provide evidence for a differential effect of HIF-1α and HIF-2α, at the molecular level, in LMPPs and Pro-T/NK in low O_2 conditions. In a hypoxic environment, HIF-1α appears necessary to enforce the lymphoid program of LMPPs while HIF-2α seems rather more important in Pro-T/NK cells.

Silencing of *HIF-1A* and *HIF-2A* impairs lymphoid development from LMPPs and Pro-T/NK

We showed that HIF-1α and HIF-2α proteins are stabilized (Figures 4D and S4D) and that HIF-1α and/or HIF-2α target genes such as *GLUT-3* (HIF-1α) (Kuang et al., 2017), *HES1* (HIF-2α) (Rouault-Pierre et al., 2013) and *VEGF* and *CXCR4* (common targets of HIF-1α and HIF-2α) (Fang et al., 2009; Rouault-Pierre et al., 2013) are induced in LMPPs and/or Pro-T/NK cells under hypoxic condition (Figures 4E and 5E). To determine to which extent HIF-1α and/or HIF-2α are important players in the lymphoid development potentials of LMPPs and Pro-TNK in low O_2 levels, we studied the functional consequences of HIF-1α KD and HIF-2α KD in LMPPs and Pro-T/NK cells. Cells were first transduced with shHIF-1α or shHIF-2α lentiviral vectors, then total or FACS-sorted HIF/KD (GFP^+) cells were kept in low O_2 concentrations before HIF/KD LMPP/Pro-T/NK-derived cells were tested either *in vitro* using lymphoid culture conditions in normoxia or *in vivo* after transplantation in NSG-W41 mice (Figure S4A). No difference in the proportion of $CD56^+$ NK cells generated from hypoxic Pro-T/NK and LMPP transduced with shHIF-1α, shHIF-2α or CTL vectors was observed (Figures 6A and 6B, left panels). However *HIF-2A* but not *HIF-1A* silencing affected NK cell production capacity from both Pro-T/NK and LMPPs (Figures 6A and 6B, right panels) to be related to a drastic decrease in NK cell precursor frequencies in Pro-T/NK (Figures S5A). Regarding *in vitro* B cell differentiation/production, no significant difference in the proportion and numbers of $CD10^+CD19^+$ B cells was observed from hypoxic LMPPs transduced with shHIF-1α or CTL vectors (Figure 6C). On the contrary, B cell differentiation potential and production capacity from LMPPs was dramatically affected by *HIF-2A* silencing (Figure 6C). Finally, HIF-2α deletion also impacted T cell generation capacity from lymphoid progenitors (Figure S5B). Interestingly, because *HIF-2A* silencing in LMPPs did not affect HIF-1α expression (Figure S4D) one can assume that NK, B and T cells changes seen with HIF-2α KD could attest of a crucial role of HIF-2α regarding survival/growth probably independently of the action of HIF-1α. Taken together, these results indicate that in contrast to *HIF-1A*

326 silencing, *HIF-2A* silencing affects lymphoid cell productions independently of the lymphoid progenitor
327 cell of origin.
328 Taken as a whole, the results indicate that hypoxia empowered *in vitro* development of lymphoid B cells
329 from LMPPs (Figure 3) and enhanced B cell lymphoid gene profile compared to normoxia/hyperoxia
330 (Figure 4). In line with these results, HIF-1α KD negatively interfered with lymphoid molecular signature
331 (Figure 5) but surprisingly did not impact *in vitro* B cell differentiation potential and production from
332 LMPPs (Figure 6). Because *in vitro* cultures may not reproduce physiologic B cell development, we
333 studied to which extent silencing of *HIF-1A* in these cells could disturb human B cell lymphopoiesis
334 obtained from NSG-W41 humanized mice after cell transplantation (Figure S4A). No difference in the
335 human $CD45^+$ cell levels was found between shCTL or shHIF-1α transduced LMPPs cells (Figure 7A).
336 Higher percentages of GFP^+ cells among $hCD45^+$ cells were generated from HIF-1α KD LMPPs (mean ±
337 SEM: 65% ± 4.4% *vs* 42.7% ± 4.9% in HIF-1α KD and CTL conditions respectively) (Figure S5C)
338 despite no such differences were observed in the initial transduction efficiencies (mean ± SEM: 70% ±
339 7.8% *vs* 62.8% ± 7.7% GFP^+ cells in HIF-1α KD and CTL conditions respectively). As LMPP-derived
340 $CD34^+$ cells proliferate less in hypoxic vs normoxic atmosphere it is possible that these *in vivo* results are
341 to be related to a release of HIF-1α KD LMPPs from quiescence imprinted by the hypoxic BM
342 environment. Nevertheless the absolute numbers of $hCD45^+GFP^+$ cells were equivalent in CTL and HIF-
343 1α KD mice (Figure 7B) indicating that maintenance of human $CD45^+$ cell production from LMPPs *in*
344 *vivo* is independent of HIF-1α. Interestingly, HIF-1α KD in LMPPs reduced $hCD45^+CD10^+CD19^+$ pre-B
345 cell levels (43.5% ±6.6% *vs* 55.3% ± 4.6% in HIF-1α KD and CTL) while it increased the proportion of
346 immature $hCD45^+CD10^+CD19^-$ pro-B cells (50% ± 9% and 38.6% ± 4.5% from shHIF-1α and shCTL
347 respectively, Figure 7C). Together with the hematopoietic recovery observed with HIF-1α KD LMPPs
348 (Figure 7B), this result reveals a significant increase of $CD10^+CD19^-$ pro-B cell numbers (Figure 7D).
349 Such results were not observed with $hCD45^+GFP^-$ LMPP-derived cells as no difference in terms of B cell
350 differentiation potential and production was observed (Figure S5D) further supporting the impact of *HIF-*
351 *1A* silencing in the *in vivo* B cell lymphoid differentiation of LMPP-derived cells. These last results reveal
352 that HIF-1α modulates *in vivo* B cell differentiation potential of LMPPs.
353 Taken altogether these findings uncover differential requirements of hypoxia and HIF-1/2α factors in the
354 early stages of human lymphopoiesis (Figure 7E).

Discussion

This study was designed to explore the role of low O_2 doses on early human lymphoid progenitors which remained largely unknown**.** Indeed the impact of hypoxic bone marrow microenvironments in the expansion and differentiation of hematopoietic progenitors, especially of the lymphoid lineage, is still elusive and mostly addressed so far in mice. Likewise the availability of *Hif-1a* and *Hif-2a* deficient or conditionally deficient mice has allowed exploring their respective role in the mouse HSPC compartment (Guitart et al., 2013; Halvarsson et al., 2017; Krock et al., 2015; Vukovic et al., 2016). In human, addressing the role of hypoxia is possible and it relies mainly on *in vitro* conditions.

In the first part of our work we observed cell proliferation inhibition and quiescence from human HPCs under hypoxia consistent with previous findings from human $CD34^+$ cells (Hermitte et al., 2006; Ianniciello et al., 2017; Shima et al., 2009; Shima et al., 2010). Early hemato-lymphoid progenitors exposed to O_2 low doses revealed a decrease in autophagy and in mitochondrial activity. This observation could underline some variances between human and mouse models, depending on the cells of origin. Indeed, autophagy levels do not interfere with cell behavior exposed to low O_2 doses in human total $CD34^+$ cells (Ianniciello et al., 2017). In mouse increase in the basal autophagy level was detected in old HSCs (Warr et al., 2013) whereas mature lymphoid cells, and most of the lymphoid progenitors presented a decrease in autophagy (Ho et al., 2017). Murine LT-HSCs are localized in a distinct population of cells characterized by low mitochondrial potential (Simsek et al., 2010) and HSC-deficient autophagy are enriched in more active mitochondria (Ho et al., 2017). This suggests, in our hands, metabolic features of UCB-isolated HPCs submitted to hypoxia, underlining their adaptability and the intrinsic properties of fetal/neonatal HPCs that could be assimilated to resting cells which are not under stress-induced hematopoiesis and thus not need to activate autophagy neither mitochondrial potential in this condition.

We then explored the functional and developmental attributes of UCB-derived HPC subtypes upon low O_2 doses and demonstrated that 3.5% O_2 differentially impacts the functionality of these cells. Particularly, hypoxia empowers *in vitro* NK-, B- and T-cell development capability from LMPPs and NK as well as T-cell potentials from Pro-T/NK cells in comparison to normoxic condition, allowing them to preserve their native intrinsic lymphoid cell generation capacity. However, in our hands, effects of low O_2 doses on *in vitro* B cell differentiation from Pro-B cells was ineffective, probably because the co-culture conditions are not optimal to reveal efficient B cell potential from these progenitors. Furthermore, one may also wonder whether hypoxia impacts also the MS-5-stromal cells, thus indirectly affecting pro-B cell progenitors. Interestingly, supernatant recovered from hypoxia-treated MS-5 cells, did not impact HSPCs, indicating no release of stromal-derived impacting secreted factors. Furthermore we observed that co-

culture of human hemato-lymphoid progenitors with stromal cells is a prerequisite to avoid loss of their potential (data not shown).

Enhancement of B-cell lymphoid development from LMPPs by hypoxia was observed *ex-vivo* and *in vivo* using transplantation in immunodeficient mice. Importantly these findings are consistent with the molecular lymphoid signatures observed from lymphoid progenitor cells under hypoxia. Particularly, enhanced *FLT3* expression in LMPPs and Pro-T/NK cells under hypoxia meets results indicating up-regulation of *FLT3* in engrafted $Lin^-CD34^+CD38^-$ cells after they acquired a hypoxic state *in vivo* (Shima et al., 2010). However studying the overall human multilymphoid cell development, including T and NK cell development, of human lymphoid LMPP and pro-T/NK progenitors in immunodeficient mice is still hardly achievable, probably due to low migration of these cells in the thymus and/or lack of compatible human cytokines. Therefore rigorous exploration of *in vivo* T and NK lymphoid potentials from LMPPs submitted to O_2 low doses is still pending, waiting for the settlement of optimized xenograft models (Doulatov et al., 2012; Renoux et al., 2015).

In the last part of the study we investigated the molecular and developmental responses of human multilymphoid progenitors targeted by HIF deletion. Indeed, differential effects of HIF-1α and HIF-2α have previously been shown in murine immune cells (Cramer et al., 2003; Dang et al., 2011; Doedens et al., 2013; Meng et al., 2018) and we wondered whether this could be the case for the human HPCs we studied. We showed that *HIF-1A* silencing in LMPPs correlated with down-regulation of early lymphoid gene expression we found to be up-regulated in low compared to high O_2 levels. Conversely, in Pro-T/NK cells, it was *HIF-2A* silencing that impacted expression of specific lymphoid genes. Inasmuch as HIF-1α KD led to *FLT3* overexpression in Pro-T/NK, an effect that was not observed when *HIF-2A* is silenced, we can hypothesize that within hypoxic Pro-T/NK, there is an interplay between HIF-1α and HIF-2α. More obvious was the behavior of *IL-15RA* expression in HIF-1α KD LMPP and Pro-T/NK cells and in HIF-2α KD Pro-T/NK which suggests that HIF-2α could play a more prominent role in Pro-T/NK than in LMPPs. These observations indicate that HIF-1α depletion in Pro-T/NK may favor a compensation process through HIF-2α stabilization outlining a potential competition between these two factors regarding early lymphoid molecular programs in line with recent findings on the contribution of these two factors in the recovery from anemia in the mouse model (Tsuboi et al., 2015). These results may rely on the control of HIF-1α and HIF-2α stability under hypoxia by a common signaling axis (Joshi et al., 2014). Furthermore, the fact that LMPPs and Pro-T/NK lacking HIF-1α can produce normal levels of lymphoid cells *in vitro* and that normal number of human $CD45^+$ cells are produced from HIF-1α deficient LMPPs *in vivo* meets recent observations underlining that HIF-1α does not impact adult murine HSCs biological functions (Vukovic et al., 2016).

Interestingly, functional analyses revealed that only *HIF-2A* silencing could preclude lymphoid cell production or differentiation of LMPPs and Pro-T/NK. This inefficient development of lymphoid cells from LMPPs and Pro-T/NK could attest of a crucial role of HIF-2α in cell survival/growth regardless the nature of the lymphoid progenitors. This assumption is in line with recent findings establishing that silencing of *HIF-2A* impairs human short- and long-term repopulating cells by increasing the endoplasmic reticulum stress induced by elevated ROS and affecting mitochondrial homeostasis, leading to early apoptosis (Rouault-Pierre et al., 2013). However the work by Guitart *et al*., shows that HIF-2α deletion does not modify murine HSPC numbers or steady-state hematopoiesis (Guitart et al., 2013) and the report by Meng *et al.* reveals that conditional deletion of HIF-2α has no essential role during murine B cell development (Meng et al., 2018) underlining here some discrepancies between human and mouse hematopoietic development probably due to different experimental systems.

Nevertheless, the fact remains that, in LMPPs, no effect of HIF-1α knockdown was noted upon *in vitro* B-cell differentiation, perhaps because B cell differentiation cultures were conducted in normoxia, allowing the LMPP-derived cells to recover a proliferation capacity and/or because LMPPs are heterogenous and B cells are produced *in vitro* from specific progenitor cell subpopulations selected over the coculture period with MS-5 stromal cells. In line with these findings no change in the absolute numbers of differentiated $CD10^+CD19^+$ B cells appeared from these HIF-1α depleted LMPPs *in vivo*. These observations could be related to the partial (or leakiness) HIF-1α knockdown in LMPPs that may still allow these cells to display B cell potential variations *in vivo,* but maybe also to the medullar hypoxic microenvironment in which production of B cells from LMPPs may arise from different cell subsets, able to find their appropriate niche in the mouse BM. Furthermore one can also hypothesize that physiological hypoxia does not disturb the final output of HIF-1α depleted $CD19^+$ B cells. On the contrary, HIF-1α knockdown in LMPPs delayed B cell differentiation *in vivo* in the NSG-W41 mouse BM, inducing an accumulation of early $CD10^+CD19^-$ B cells. These latter results are in favor of a substantial role of HIF-1α in B cell lymphoid development of LMPPs in hypoxia, a finding consistent with the significant down-regulation of *SOX4*, *BCL11A* and *E2A* expression in these HIF1α KD cells in hypoxia (Laurenti et al., 2013).

The results implying the involvement of HIF-1α in early B lymphopoiesis are in line with the work by Kojima *et al.*, based on *Hif-1α*$^{-/-}$→*Rag2*$^{-/-}$ chimeric mice model in which HIF-1α was shown to be an essential factor for B cell development in bone marrow allowing transition from late pro-B cells to pre-B cells (Kojima et al., 2002; Kojima et al., 2010). Our results are also corroborated by recent findings based on conditional deletion of *Hif-1α* or *Hif-2α* in B cells at late developmental stages showing that only Hif-1α regulates $CD1d^{hi}CD5^+$ B cell expansion and represents a critical node involved in IL-10 production by B cells (Meng et al., 2018).

In conclusion, multi-lymphoid progenitors submitted to low O_2 doses may represent a relevant indication for the exploration of the relationship between human early hemato-lymphoid progenitor cells and their microenvironment. This would contribute to set the BM niche at heart of the early stages of human lymphopoiesis allowing establishing valuable tools for exploring early cellular and molecular events that direct the initiation of normal and pathological lymphoid cell fate.

Acknowledgements

We acknowledge the midwives from Clinique des Noriets in Vitry-sur-Seine and the Cell therapy department of Hôpital Saint Louis in Paris, France, especially Prof J. Larghero, for their devotion in providing cord blood samples free of charge and the families who accepted to donate the samples for research purposes. This work was made possible thanks to several in-house platforms (Flow cytometry, Microscopy, Irradiation and animal facilities) of IRCM, Fontenay-aux-Roses, France. We are thus grateful to J. Tilliet, V. Barroca, S. Vincent-Naulleau, N. Dechamps and J. Bajer for their great help during this project. A special thank to P. Fouchet (IRCM, LDG, Fontenay aux Roses) for helping with the hypoxia chamber and G. Piton (CIGEX platform, IRCM) for the lentivector productions. We also acknowledge Laurent Renou for daily help and informatic assistance and Elia Henry for helping in processing cord blood samples. We are indebted with C. Waskow and S. Rahmig for their help in starting a NSG-W41 mouse colony and to PH Roméo for his great input during the writing of the manuscript. This study was supported by grants from INSERM, CEA, University Paris Diderot and University Paris Sud, Ligue Nationale contre le Cancer (équipe labellisée up to 2017) and Fondation ARC pour la recherche sur le cancer (équipe labellisée from 2018), Association Laurette Fugain and Agence Nationale pour la Recherche. SC, RH, FM and FP are part of Micronit GDR.

Author Contribution: S.C. designed and performed experiments, contributed to all aspects of the work, analyzed data and participated in writing the manuscript. B.U. performed *in vivo* experiments. I.N. supervised the molecular experimental design and helped in experiments. J.R. helped with confocal microscopy analysis. L.F., J.C., M-L.A., F.M. participated in experiments. F.P. supervised the *in vivo* transplantation assays, discussed the results and helped writing the manuscript. R.H. provided the conceptual framework of the research, set up the methodological strategy, performed experiments, analyzed data and wrote the manuscript.

Declaration of Interests

The authors declare no competing interests.

Figure Legends

Figure 1. Cellular and phenotypic metabolic profiles of HPC-derived co-culture cells under 21% O_2 and 3.5% O_2.

(A) Representation of pathways of lymphoid development from HSPC, MPP, LMPP and ELP.

(B) General experimental strategy: HPCs were co-cultured under 21% or 3.5% O_2 with MS-5 stromal cells. Co-cultures were sacrificed at day 7 and HPC-derived cells (Figure 1B) were analyzed *in vitro* for their NK, B and T cell differentiation capacity in limiting dilution assay (LDA) and bulk conditions (a day-0 lymphoid differentiation from non-co-cultured HPCs was used as a control), at the molecular level by qRT-PCR and *in vivo* in NSG-W41 immunodeficient mice.

(C) and **(D)** $CD34^+$ cell percentages and absolute numbers among co-culture derived-cells in 21% O_2 and 3.5% O_2 conditions (n = 10 for HSPCs, MPPs, LMPPs and Pro-T/NK and n = 4 for Pro-B).

(E) Percentages of Annexin V^+ apoptotic cells among $CD34^+$ cells derived from HPC co-cultures under 21% O_2 and 3.5% O_2 (n = 3-4).

(F) Percentages of proliferative $Ki67^+$ cells among $CD34^+$ cells derived from HPC co-cultures under 21% O_2 and 3.5% O_2 (n = 4).

(G) Cell cycle analysis of $CD34^+$ cells derived from HPC co-cultures under 21% O_2 and 3.5% O_2 (n = 4).

(H) Autophagy profile of $CD34^+$ cells derived from HPC co-cultures under 21% O_2 and 3.5% O_2. Panel displays MFI values of Cyto-ID staining (n = 4-7).

(I) Measurement of mitochondrial transmembrane potential and mass. HSPCs, MPPs, LMPPs and Pro-T/NK were co-cultured under 21% O_2 or 3.5% O_2 with MS-5 stromal cells. Co-cultures were sacrificed at day-7 and HPC-derived $CD34^+$cells were analyzed according to Tetramethylrosamine ethyl ester (TMRE) and Mitotracker (MTG) stainings. Low ratio of MFI indicates low mitochondrial activity. Results are shown as the mean ± SEM (n represents number of independent experiments), *p < 0.05, **p < 0.01, ***p < 0.001. MFI: mean fluorescence intensity. See also Figure S1.

Figure 2. NK, B and T cell precursor frequencies among HPC-derived cells under 21% O_2 and 3.5% O_2.

(A) Comparative analysis of day-0 HPCs and HPC co-cultures-derived cells from 21% O_2 and 3.5% O_2 conditions in limiting-dilution assays under NK condition cultures (1 experiment out of 3 for HSPCs, MPPs and Pro-T/NK and 1 experiment out of 2 for LMPPs are shown here).

(B) Same as in (A) but in B condition cultures (1 experiment out of 2 for HSPCs, MPPs and LMPPs is shown here).

(C) Same as in (A) but in T condition cultures (1 experiment out of 2 for LMPPs and Pro-T/NK is shown here). Note that T cell precursor frequencies among LMPP and Pro-T/NK derived cells were analyzed for the presence of total $CD7^+$ T cells and the presence of $CD7^+CD4^+CD8^-CD3^-$ ISP cells and/or $CD7^+CD4^+CD8^+$ DP cells and/or $CD7^+CD4^-CD8^+CD3^+$ or $CD7^+CD4^+CD8^-CD3^+$ committed T cells (see Figure S2A for phenotypic analysis strategy). Wells were scored as positive for NK, B or T cells when % of lymphoid cells was ≥ 1% and represent homogeneous population. 95% confidence intervals are indicated in Figure S2C. *p<0.05, **p<0.01, ***p<0.001 ****p<0.0001, ns: no significant. See also Figures S2 and S3.

Figure 3. *In vivo* analysis of LMPPs following 21% O_2 and 3.5% O_2 treatments.

Sorted LMPPs were co-cultured under 21% O_2 and 3.5% O_2 with MS-5 stromal cells. Co-cultures were sacrificed at day-7 and $30x10^3$ LMPP-derived cells were injected into one femur of NSG-W41 mice without irradiation, $30x10^3$ day-0 non-manipulated LMPPs were used as control. Bone marrows were analyzed 2 weeks after injection for co-cultures-derived cells and 3 weeks after injection for day-0 cells (Figure S1). Shown are results from n = 6-9 mice/condition, 2 independent experiments.

(A) Percentage of $hCD45^+$ cells (chimerism) in BM of NSG-W41 mice injected with day-0 control LMPPs or LMPP-derived cells from 21% O_2 and 3.5% O_2 co-cultures.

(B) Percentage of human $CD14^+/CD15^+/CD33^+$ myeloid and $CD19^+$ B lymphoid cells in BM of NSG-W41 mice injected with day-0 control LMPPs and LMPP-derived cells from 21% O_2 and 3.5% O_2 co-cultures.

(C) Human B cell absolute numbers from BM of NSG-W41 mice injected with day-0 control LMPPs or LMPP-derived cells from 21% O_2 and 3.5% O_2 co-cultures.

Dot plots in A and B show representative phenotypic profiles for chimerism and lympho-myeloid differentiation of BM from injected leg. Results are shown as the median and mean ± SEM, *p < 0.05, **p < 0.01.

Figure 4. Molecular analysis of LMPPs and Pro-T/NK cells under 3.5% O_2.

(A) Relative gene expression in LMPPs after co-cultures under 21% O_2 and 3.5% O_2 condition (n = 8).

(B) Relative gene expression in Pro-T/NK after co-cultures under 21% O_2 and 3.5% O_2 condition (n = 8).

(C) *HIF-1α* gene expressions in LMPPs and Pro-T/NK cells after co-cultures under 21%O_2 and 3.5% O_2 condition (n = 8).

(D) HIF-1α protein expression. Cells derived from LMPPs and Pro-TNK cells co-cultured under 21% O_2 and 3.5% O_2 for 7 days were stained with anti-human CD45 (green) and anti-human HIF-1α (red) and counterstained with DAPI. Cells were then analyzed by Leica TCS SP8 MP Confocal Microscope (Leica,

Germany). (original magnification 63x, scale bar represents 7.5µM). Presence of HIF-1α protein in the nucleus is indicated by the colocalisation coefficient (R) (n = 50 cells).

(E) Expressions of *VEGFA*, *CXCR4* and *GLUT3* HIF-1α target genes in LMPPs and Pro-T/NK cells after co-cultures under 21% O_2 and 3.5% O_2 condition (n = 8).

For RT-QPCR experiments, gene expression was normalized to the housekeeping gene *β2M* and data are expressed relative to 21% O_2 condition. Results are shown as the mean ± SEM. *p < 0.05, **p < 0.01, ***p < 0.001.

Figure 5. Expression of *HIF* genes and analysis of their knockdown in LMPPs and Pro-T/NK cells under 3.5% O_2.

LMPPs and Pro-T/NK cells were transduced with shCTL or shHIF-1α vectors for 48 hr, and co-cultured under 3.5% with MS-5 stromal cells for 2 days. After the co-culture period, HPC-derived cells were analyzed at the molecular level.

(A) Relative *HIF-1A* expressions in cells derived from LMPPs and Pro-T/NK after transduction with shHIF-1α followed by a 3.5% O_2 treatment (n = 4).

(B) Relative *HIF-2A* and *VEGFA* expressions in transduced LMPP and Pro-T/NK-derived cells (n = 4).

(C) Lymphoid gene expressions analysis in transduced LMPP and Pro-T/NK-derived cells (n = 4).

(D) Relative *HIF-1A* and *HIF-2A* expression in transduced Pro-TNK-derived cells (n = 4).

(E) Relative *VEGFA*, *GLUT3, CXCR4* (n = 4) and *HES1* (n = 3) expression in transduced Pro-TNK-derived cells.

(F) Relative lymphoid gene expressions in transduced Pro-T/NK-derived cells (n = 4-5).

Results are shown as the mean ± SEM. *p < 0.05, **p < 0.01, ***p < 0.001. Gene expression was normalized to *β2M* gene and data are expressed relative to shCTL under 3.5% O_2 culture condition (n = 3-5 independent experiments). See also Figure S4.

Figure 6. *In vitro* functional consequences of *HIF* genes KD in LMPPs and Pro-T/NK under 3.5% O_2.

LMPPs and Pro-T/NK cells were transduced with shCTL, shHIF-1α or shHIF-2α vectors for 48 hr. Sorted GFP^+ cells were co-cultured for 4 days with MS-5 stromal under 3.5% O_2. After the co-culture period, LMPP- or Pro-T/NK-derived cells were submitted to NK and/or B cell differentiation.

(A) Bulk cultures in NK conditions from transduced Pro-T/NK-derived cells. NK cell percentages and absolute numbers are shown (n = 3).

(B) Bulk cultures in NK conditions from transduced LMPP-derived cells. NK cell percentages and absolute numbers are shown ($n = 3$).

(C) Bulk cultures in B conditions from transduced LMPP-derived cells. $CD10^+CD19^+$ B cell percentages and absolute numbers are shown ($n = 3$).

One representative phenotypic analysis of NK or B cell differentiation is shown here. Results are shown as the mean ± SEM, *n* represents number of independent experiments, *p < 0.05, **p < 0.01. See also Figures S4 and S5.

Figure 7. *In vivo* functional consequences of HIF genes KD in LMPPs under 3.5% O_2.

(A) Percentages of $hCD45^+$ cells (chimerism) in BM of NSG-W41 mice injected with shCTL and shHIF-1α transduced LMPP cells after a period of 3.5% O_2 treatment.

(B) $hCD45^+GFP^+$ absolute numbers in BM of NSG-W41 mice injected with shCTL and shHIF-1α transduced LMPP cells after a period of 3.5% O_2 treatment.

(C) Percentages of $hCD10^+CD19^+$ and $hCD10^+CD19^-$ B cells among $hCD45^+GFP^+$ cells.

(D) Human $CD10^+CD19^+$ and $CD10^+CD19^-$ B cells absolute numbers among $hCD45^+GFP^+$ from BM of NSG-W41 mice injected with shCTL and shHIF-1α transduced LMPP-derived cells after a period of 3.5% O_2 treatment. Plots in B and D show representative phenotypic profiles for chimerism and B lymphoid differentiation of BM from injected legs (12-13 mice/condition, $n = 3$). Results are shown as median, *p < 0.05, **p < 0.01, ns: no significant, dot plots illustrate results from one representative mouse.

(E) Possible role of hypoxia and HIFs in regulation of human early lymphopoiesis. Hypoxia allows LMPPs and Pro-T/NK to exhibit or maintain their lymphoid potential in comparison to normoxia condition or to native cells. At the molecular level, HIF-1α seems to act preferentially on LMPPs while HIF-2 α appears more specific to Pro-T/NK. At the functional level, HIF-1α is required for *in vivo* early B cell development from LMPPs and HIF-2α is critical for lymphoid cell generation. See also Figure S4 and S5.

STAR Methods

Lead Contact and Materials Availability

Further information and requests for resources should be directed to and will be fulfilled by the Lead Contact, Rima Haddad (rima.haddad@u-psud.fr; rima.haddad@universite-paris-saclay.fr).

Materials Availability Statement

This study did not generate new unique reagents.

Experimental Model and Subject details

Mice

NOD.Cg-*Prkdc*^{scid} *Il2rg*^{tm1Wjl}/SzJ *Kit*$^{W41/W41}$ female mice (abbreviated NSG-W41) (Cosgun et al., 2014) were kindly provided by Susann Rahmig and Claudia Waskow, Technical University Dresden, Dresden, Germany. Mice were produced and housed in pathogen-free animal facilities at CEA (Fontenay-aux-Roses, France). Experimental procedures were performed in compliance with the French Agriculture Ministry and local ethics committee regulations (Authorization number 9458-2017033110277117).

Human umbilical cord blood samples

Normal UCB units from male or female new born were collected according to institutional guidelines and with the informed written consent of the mothers. UCB samplings and experiments described here were done in accordance with a signed authorization from Clinique des Noriets (Vitry-sur-Seine, France) advisory board and from the Laboratory of cell therapy of Hospital Saint Louis (Paris, France).

Cell lines

Mouse bone marrow stromal MS-5 cells were originally obtained from Dr K Mori (Nagata University, Japan), and MS-5/ huDelta-like1(DLL1) cells have been described in Armstrong *et al*. (Armstrong et al., 2009). MS5 cells were transduced with lentiviral TRIP-ΔU3-EF1α-DLL1–IRES-GFP or TRIP-ΔU3-EF1α-GFP vectors (Sirven et al., 2000) such that they were 100% GFP$^+$ by fluorescence-activated cell sorter (FACS). The human *dl1* cDNA was originally kindly provided by Dr E. Parreira (Gulbenkian Instituto, Lisboa, Portugal).These cell lines were grown in complete alpha-MEM containing 10% FCS (Invitrogen, Cergy Pontoise, France and Sigma-Aldrich®, St Louis, MO).

649

650 **Primary cell cultures**

651 Cultures of UCB-derived $CD34^+$ hematopoietic progenitors were conducted as described in "Method
652 details" section.

653

654 ## Method details

655 **Flow cytometry analysis**

656 Immunolabeling of cells was performed by incubating the cells for 30 min at 4°C in phosphate-buffered
657 saline (PBS, ThermoFisher Scientific) or directly in cell suspension medium (for LDA analysis) with
658 human specific mouse monoclonal antibodies (mAbs) (1:100 final) provided in supporting informations
659 (Table S1). Analysis of labeled cells was conducted using BD SORP LSR II and BD FACSCanto (BD
660 Bioscience). Analyses of raw data were performed using FlowJo software (Treestar, Ashland, OR).

661

662 **Human UCB-derived HPCs - cell sorting**

663 Following ficoll separation (Lymphocytes separation medium, Eurobio, les Ulis, France), $CD34^+$ cells
664 were purified by immunomagnetic selection using a CD34 MicroBeads kit (Miltenyi Biotec, Paris,
665 France). For isolation of $CD34^+CD38^{lo/-}CD45RA^-CD90^+$ HSPCs, $CD34^+CD38^{lo/-}CD45RA^-CD90^-$ MPPs,
666 $CD34^+CD45RA^{hi}CD7/CD10/CD19^-CD62L^+$ LMPPs, $CD34^+CD45RA^{hi}CD7^+$ Pro-T/NK and
667 $CD34^+CD45RA^{hi}CD7/19^-CD10^+$ Pro-B cells, purified $CD34^+$ cells, pooled from different UCB samples,
668 were incubated for 30 min at 4°C in PBS with anti-human CD34-PerCP-Cy5.5, CD38-APC-H7,
669 CD45RA-PE, CD90-BV421, CD7-APC, CD10-FITC, CD19-FITC or CD19-APCH7, CD62L-PECy7
670 mAbs (mAbs are listed in Table S1) at 1:100 final in presence of Hoechst or Zombie Aqua™ (BioLegend)
671 viability dyes. Then, HPCs were sorted, using a BD Influx™ cell sorter (Becton Dickinson, Mountain
672 View, CA). Purity of sorted HPC populations was > 90%.

673

674 **Primary co-cultures under normoxia (21% O_2) and hypoxia (3.5% O_2)**

675 MS-5 cells were plated at $3x10^4$ cells/cm^2 24h-48h in complete alpha-MEM containing 10% FCS before
676 co-culture initiation. FACS-sorted $CD34^+CD38^{lo/-}CD45RA^-CD90^+$ HSPCs, $CD34^+CD38^{lo/-}CD45RA^-$
677 $CD90^-$ MPPs, $CD34^+CD45RA^{hi}CD7/CD10/CD19^-CD62L^+$ LMPPs, $CD34^+CD45RA^{hi}CD7^+$ Pro-T/NK
678 ($5x10^3$-10^4 cells/cm^2) and $CD34^+CD45RA^{hi}CD7/19^-CD10^+$ Pro-B (300-500 cells/cm^2) were co-cultured
679 during 7 days with MS-5 cells under 3.5% O_2 (PrOox culture chamber BioSpherix, Ltd, Redfield, NY)
680 and 21% O_2 in standard complete H5100 human long-term culture medium (StemCell Technologies,
681 Grenoble, France) in 24 well plates (Dutscher, Issy les Moulineaux, France). At the end of the culture

period, cells were counted and analyzed phenotypically and functionally.

Cell cycle and Apoptosis

Ki-67/Hoechst-7AAD

Cells derived from primary co-cultures under normoxia and hypoxia were first incubated with anti-human CD34-APC mAb (Biolegend) as described and washed with PBS. Then cells were stained with Ki67-PE antibody (BD, 556027) and Hoechst 33342 (Invitrogen) or 7AAD (Beckman Coulter) using the Fixation/Permeabilization kit Cytofix/Cytoperm™ (554714, BD) according to the manufacturer's instructions. In brief, cells were fixed in 100 µL of Fixation and Permeabilization solution, mixed, incubated for 15 min at 4°C and washed with 1 mL of Perm/Wash 1X. Cells were then resuspended in 100 µL of Perm/Wash 1X and incubated with 3 µL Ki67-PE antibody for 45 min at 4°C. 10 min before the end of the incubation, 7AAD or Hoechst were added and cells were washed with 1 mL of Perm/Wash 1X and resuspended in PBS. Analyses were conducted by flow cytometry.

Annexin V staining

Cells derived from primary co-cultures under normoxia and hypoxia were stained with CD34-PE mAb, washed twice with cold PBS and incubated for 15 min at room temperature in Annexin V buffer 1X (BD, 51-66121E) containing Annexin V-APC (550475, BD). Apoptotic cells were determined by flow cytometry after addition of 7AAD.

Autophagy analysis

Cells derived from primary co-cultures under hypoxia and normoxia were washed and resuspended in PBS, FCS 5% and stained with CD34-APC mAb and Cyto-ID® Green autophagy dye (1/2000), according to the manufacturer's instructions (Cyto-ID® Autophagy detection kit, Enzo Life Sciences, ENZ-51031, Villeurbanne, France). Rapamycin (500 nM, Thermofisher Scientific) and Chloroquine (10 µM, Sigma-Aldrich®) treatments were used as positive controls. At the end of the incubation cells were washed and resuspended in PBS and Hoechst 33258 (Invitrogen). Analyses were done by flow cytometry.

Quantification of mitochondria mass and membrane potential

Cells derived from primary co-cultures under hypoxia and normoxia were incubated with 50 nM Mitotracker Green (MTG, M7514, ThermoFisher Scientific) and 100 nM TetraMethylRhodamine methyl Ester (TMRE, T669, ThermoFisher Scientific) for 30 min at 37°C. Negative control cells consisted in

MTG+TMRE treated cells incubated with Carbonyl cyanide 4-(trifluoromethoxy) phenylhydrazone (FCCP, 2920, Sigma-Aldrich®) at 50 µM during 15 min before the end of the staining process. Analyses were done by flow cytometry. The corrected values correspond to MFI of treated cells minus MFI of FCCP negative control. When needed, cells were treated for 10 min at 37°C in the presence or absence of verapamil (50 µM, V-4629, Sigma-Aldrich®) before MTG labelling at 37°C for additional 30 min, washed in 1×PBS and centrifuged at 1200 rpm for 5 min at 4°C as previously described (de Almeida et al., 2017).

Immunofluorescence and confocal microscopy

At the end of the co-culture period under normoxia and hypoxia, cells (10^4-$2x10^4$) were washed and fixed in 4% paraformaldehyde for 15 min at room temperature and bathed consecutively in cold absolute ethanol for 20 min at -20°C and in PBS for 30 min at room temperature. Cells were layered on poly-l-lysine treated slides (Sigma-Aldrich®) and incubated for 3 hr at 4°C then washed three times in PBS. Slides were then incubated for 15 min in PBS, 0.2% Triton (Sigma-Aldrich®),washed three times in PBS and blocked 1 hour in PBS, 3% BSA, 0.1% Tween® 20 (Sigma-Aldrich®) before incubation over night at 4°C with the following primary mAbs: mouse anti-human CD45 (1/250, clone HI30, BD Biosciences) and rabbit anti-human HIF-1α (1/250, Abcam, ab51608) or rabbit anti-human HIF-2α (1/250, Abcam, ab207607). Then, cells were washed with PBS, 0.2% Tween-20 and incubated in PBS, 0.2% Tween-20 for 90 min at room temperature in the dark with the following secondary antibodies: goat anti-mouse-DyLight®488 (1/200, Bethyl Laboratories) and goat anti-rabbit-AlexaFluor®594 (1/200, ThermoFisher Scientific). Negative controls were cells incubated without primary mAbs and concentration-matched secondary antibodies. Slides were counterstained with 4',6-diamidino-2-phenylindole, dihydrochloride (DAPI) at 1/2000.

Cells were analyzed by a Leica TCS SP8 MP Confocal Microscope (Leica, Germany). Images were acquired at 63X, and analyzed with the ImageJ software (Larbi et al., 2014). Co-localisation coefficient (R) was determined by the Plugin LOCI.

Assessment of NK and B-cell differentiation potentials

Day-0 HPCs and cells derived from primary co-cultures with either MS-5 cells under normoxia or MS-5 cells under hypoxia were cultured under NK- and B-cell differentiation conditions in normoxia. For NK-cell culture conditions, cells (10^3 cells/cm^2) were co-cultured for 3 weeks with MS-5 cells, in RPMI 1640 (ThermoFisher Scientific), 5% FCS (StemCell Technologies, Grenoble, France), 10% human AB serum (Jack Boy, Toronto, Canada), with human recombinant cytokines: 50 ng/mL recombinant human stem cell

748 factor (rhSCF, Miltenyi Biotec), 5 ng/mL rhInterleukin (IL)-2, 1 ng/mL rhIL-15 (PeproTech, France)
749 (Haddad et al., 2008). B-cell differentiation of day-0 HPCs and co-cultures-derived cells was assessed by
750 growing cells (10^3-10^4 cells/cm^2) for 3 weeks in unmodified MS-5 cell-coated plates in IMDM
751 (ThermoFisher Scientific) complemented with 5% FCS, 2 mM L-Glutamine, without cytokines. Half of
752 the complete media was replaced weekly (Haddad et al., 2008). At the end of the culture period,
753 hematopoietic cells were counted and NK and B cells were identified by flow cytometry analysis of CD56
754 (NK cells) and CD19 (B cells).
755
756 **Assessment of T-cell differentiation potential**
757 Day-0 HPCs and cells derived from primary co-cultures with either MS-5 cells under normoxia or MS-5
758 cells under hypoxia ($5x10^3$-10^4 cells/cm^2) were co-cultured in normoxia in contact with MS-5/DLL1
759 ($2.8x10^4$ cells/cm^2) in reconstituted alpha-MEM (ThermoFisher Scientific) supplemented with 10% FCS
760 (StemCell Technologies and Sigma-Aldrich®) and 10% human AB serum (J Boy, Reims, France), in
761 presence of rhSCF (50 ng/mL), rhFlt3-ligand (20 ng/mL, Miltenyi Biotec), rhIL-7 (10 ng/mL, Miltenyi
762 Biotec), Insulin (20 nM, Sigma-Aldrich®) and as described (Calvo et al., 2012). Medium was half
763 changed twice a week and stromal layer was renewed once a week. At passage time point, hematopoietic
764 cells were counted and 100 µL containing cells were labelled with specific mAbs (against T cell markers:
765 CD7/CD5/CD4/CD8/CD3) when enough cells were available for FACS analysis. T cell cultures were
766 maintained up for 5 weeks.
767
768 **Limiting-dilution assays (LDA)**
769 To assess NK-, B- and T- cell progenitor frequencies, cells (day-0 HPCs and co-cultures-derived cells
770 under normoxia and hypoxia) were seeded at 300, 100, 30, 10, 3, and 1 cell(s)/well into MS-5 or MS-
771 5/DL1 cell coated 96-well plates (ATGC) and cultured as described above. Cultures lasted for 3 to 5
772 weeks with half medium changes and fresh cytokines added every 6 to 7 days. Plates were examined
773 weekly, and cell-containing wells were scored under the microscope as previously described (Haddad et
774 al., 2004). At the end of the cultures, NK, B and T cells were identified by flow cytometry analysis of
775 CD56 (NK cells), CD19 (B cells) and CD7/CD5/CD4/CD8/CD3 (T cells) expressions. The maximum
776 likelihood estimate of NK-, B-, or T-cell precursors was calculated according to the single-hit Poisson
777 model using the L-Calc™ limiting dilution analysis software from STEMCELL Technologies which also
778 provides a confidence interval (95% CI).
779
780 **Xenotransplantation**

Mice were anesthetized with isoflurane before day-0 LMPP cells and co-cultured LMPP-derived cells ($30x10^3 – 50x10^3$) were transplanted into their femurs.

After 3 weeks (for day-0 cells) and 2 weeks (for cells derived from 1 week co-cultures), the mice were euthanized by CO_2 inhalation using an infusion device (TEM SEGA, Pessac, France). After treatment by ACK lysis buffer (Thermo Fisher Scientific) the BM were analyzed by FACS for the presence of human hematopoietic cells using the conjugated mouse human mAbs listed in Table S1.

Quantitative reverse transcription PCR (QRT-PCR).

RNA samples were extracted using RNeasy® Plus Micro Kit (Qiagen, Courtaboeuf, France) according to the manufacturer's instructions and reverse transcribed into cDNA with SuperScript VILO cDNA synthesis kit (Invitrogen, Carlsbad, USA). Quantitative real time PCR was performed using the power SYBR-Green I Master Mix (Applied Biosystems, Thermo Fisher Scientific) and 0,5 µM of primers (Eurogenetec) on a 7900HT instrument fast real-time PCR system (Applied Biosystems). Raw data were obtained in terms of Ct values and normalized to the Ct values of the housekeeping gene *β2M*. Analyzed genes with the corresponding forward and reverse primer sequences (5'➔3') are listed in Table S2.

Western Blot analysis

Nuclei were extracted with lysis buffer A containing 10mM HEPES/KOH pH 7.9, 1.5 mM $MgCl_2$, 10Mm KCL, 0.5% DOC supplemented with a protease inhibitor mix (Sigma-Aldrich®). Nuclear proteins were extracted with lysis buffer C containing 20mM HEPES-KOH pH 7.9, 1.5 mM $MgCl_2$, 25% Glycerol, 0.2 mM EDTA, 420 mM NaCl, 0.5% sodium deoxycholate (Sigma-Aldrich®) supplemented with a protease inhibitor mix. Proteins were separated by 10% SDS PAGE, transferred onto nitrocellulose membrane (Schleicher & Schuell) and immunoblotted in standard conditions. Primary antibodies from rabbit were used against human HIF-1α (1/1000, ref: ab51608, Abcam), and human Lamin-B1 (1/2000, ref: ab16048, Abcam). The Secondary antibody was a goat anti-rabbit (IRDye® 800CW) (1/10000, ref: ab216773, Abcam). Analysis was done on the Odyssey® CLx Imaging System by revealing HIF-1α first and Lamin-B1 24 hrs later.

Lentiviral vectors and cell transduction.

shRNA sequences directed to *HIF-1A* (shHIF-1α: gatgttagctccctatatcccttcaagagagggatatagggagctaacatc) and *HIF-2A* (shHIF-2α : aggccgtactgtcaacctcaattcaagagattgaggttgacagtacggcct), were subcloned in the bi-cistronic lentiviral vector TRIP/ΔU3-EF1α that contains the enhanced green fluorescent protein under the

control of the EF1α promoter (pTripΔU3Ef1a-EGFPMCSΔU3) kindly provided by F. Mazurier (Rouault-Pierre et al., 2013). shRNA (aaaaagtgttgggtcgcgaaaggtctcttgaacctttcgcgacccaacacggggatc) directed against the hepatitis B virus was used as a control (shCTL).

Concentrated lentiviral supernatants were generated and collected by the CIGEX platform of CEA/IRCM Institute. LMPP and Pro-T/NK sorted cells ($40x10^3$-$50x10^3$ cells/100 µL) were incubated with concentrated virus at a multiplicity of infection of $4x10^6$-$12x10^6$ Units/mL during 48 hours in serum-free medium (BIT, ref: 09500, Stem Cell Technologies) supplemented with SCF (100 ng/mL), rhIL-3 (60 ng/mL), thrombopoietin (TPO, 50 ng/mL), and FL (100 ng/mL) purchased from Miltenyi Biotec (Brunet de la Grange et al., 2006; Laurenti et al., 2013). Cells were carefully washed after transduction, and co-cultured with MS-5 stromal cells under 3.5% O_2 before performing molecular analysis, transplantation in mice or culture assays.

Quantification and Statistical analysis

Values were presented as mean ± SEM from at least three independent experiments or median from three independent experiments for *in vivo* assays. To analyze differences in mean or variance values between low-number samples, data were statistically tested using the ANOVA test, the Mann-Whitney test (in independent cases) and the rank signed Wilcoxon test (in matched cases) with GraphPad Prism 6. For LDA, the significance of differences between groups was obtained by the comparison of the ratio of proportions using a two-tailed test provided by the L-Calc™ limiting dilution analysis software from STEMCELL Technologies. *p<0.05, **p<0.01, ***p<0.001, ****p<0.0001.

Data and Code Availability

This study did not generate/analyze datasets/code.

References

Adolfsson, J., Mansson, R., Buza-Vidas, N., Hultquist, A., Liuba, K., Jensen, C.T., Bryder, D., Yang, L., Borge, O.J., Thoren, L.A., *et al.* (2005). Identification of Flt3+ lympho-myeloid stem cells lacking erythro-megakaryocytic potential a revised road map for adult blood lineage commitment. Cell *121*, 295-306.

Aiuti, A., Tavian, M., Cipponi, A., Ficara, F., Zappone, E., Hoxie, J., Peault, B., and Bordignon, C. (1999). Expression of CXCR4, the receptor for stromal cell-derived factor-1 on fetal and adult human lympho-hematopoietic progenitors. Eur J Immunol *29*, 1823-1831.

Alhaj Hussen, K., Vu Manh, T.P., Guimiot, F., Nelson, E., Chabaane, E., Delord, M., Barbier, M., Berthault, C., Dulphy, N., Alberdi, A.J., *et al.* (2017). Molecular and Functional Characterization of

Lymphoid Progenitor Subsets Reveals a Bipartite Architecture of Human Lymphopoiesis. Immunity *47*, 680-696 e688.

Armstrong, F., Brunet de la Grange, P., Gerby, B., Rouyez, M.C., Calvo, J., Fontenay, M., Boissel, N., Dombret, H., Baruchel, A., Landman-Parker, J.*, et al.* (2009). NOTCH is a key regulator of human T-cell acute leukemia initiating cell activity. Blood *113*, 1730-1740.

Belluschi, S., Calderbank, E.F., Ciaurro, V., Pijuan-Sala, B., Santoro, A., Mende, N., Diamanti, E., Sham, K.Y.C., Wang, X., Lau, W.W.Y.*, et al.* (2018). Myelo-lymphoid lineage restriction occurs in the human haematopoietic stem cell compartment before lymphoid-primed multipotent progenitors. Nat Commun *9*, 4100.

Ben-Shoshan, J., Maysel-Auslender, S., Mor, A., Keren, G., and George, J. (2008). Hypoxia controls CD4+CD25+ regulatory T-cell homeostasis via hypoxia-inducible factor-1alpha. Eur J Immunol *38*, 2412-2418.

Berardi, A.C., Meffre, E., Pflumio, F., Katz, A., Vainchenker, W., Schiff, C., and Coulombel, L. (1997). Individual CD34+CD38lowCD19-CD10- progenitor cells from human cord blood generate B lymphocytes and granulocytes. Blood *89*, 3554-3564.

Blom, B., and Spits, H. (2006). Development of human lymphoid cells. Annu Rev Immunol *24*, 287-320.

Boos, M.D., Ramirez, K., and Kee, B.L. (2008). Extrinsic and intrinsic regulation of early natural killer cell development. Immunol Res *40*, 193-207.

Brunet de la Grange, P., Armstrong, F., Duval, V., Rouyez, M.C., Goardon, N., Romeo, P.H., and Pflumio, F. (2006). Low SCL/TAL1 expression reveals its major role in adult hematopoietic myeloid progenitors and stem cells. Blood *108*, 2998-3004.

Caldwell, C.C., Kojima, H., Lukashev, D., Armstrong, J., Farber, M., Apasov, S.G., and Sitkovsky, M.V. (2001). Differential effects of physiologically relevant hypoxic conditions on T lymphocyte development and effector functions. J Immunol *167*, 6140-6149.

Calvo, J., BenYoucef, A., Baijer, J., Rouyez, M.C., and Pflumio, F. (2012). Assessment of human multi-potent hematopoietic stem/progenitor cell potential using a single in vitro screening system. PLoS One *7*, e50495.

Chambers, S.M., Boles, N.C., Lin, K.Y., Tierney, M.P., Bowman, T.V., Bradfute, S.B., Chen, A.J., Merchant, A.A., Sirin, O., Weksberg, D.C.*, et al.* (2007). Hematopoietic fingerprints: an expression database of stem cells and their progeny. Cell Stem Cell *1*, 578-591.

Cho, S.H., Raybuck, A.L., Stengel, K., Wei, M., Beck, T.C., Volanakis, E., Thomas, J.W., Hiebert, S., Haase, V.H., and Boothby, M.R. (2016). Germinal centre hypoxia and regulation of antibody qualities by a hypoxia response system. Nature *537*, 234-238.

Chow, D.C., Wenning, L.A., Miller, W.M., and Papoutsakis, E.T. (2001). Modeling pO(2) distributions in the bone marrow hematopoietic compartment. I. Krogh's model. Biophys J *81*, 675-684.

Cipolleschi, M.G., D'Ippolito, G., Bernabei, P.A., Caporale, R., Nannini, R., Mariani, M., Fabbiani, M., Rossi-Ferrini, P., Olivotto, M., and Dello Sbarba, P. (1997). Severe hypoxia enhances the formation of

900 erythroid bursts from human cord blood cells and the maintenance of BFU-E in vitro. Exp Hematol *25*,
901 1187-1194.
902
903 Cipolleschi, M.G., Dello Sbarba, P., and Olivotto, M. (1993). The role of hypoxia in the maintenance of
904 hematopoietic stem cells. Blood *82*, 2031-2037.
905
906 Cosgun, K.N., Rahmig, S., Mende, N., Reinke, S., Hauber, I., Schafer, C., Petzold, A., Weisbach, H.,
907 Heidkamp, G., Purbojo, A.*, et al.* (2014). Kit regulates HSC engraftment across the human-mouse species
908 barrier. Cell Stem Cell *15*, 227-238.
909 Cramer, T., Yamanishi, Y., Clausen, B.E., Forster, I., Pawlinski, R., Mackman, N., Haase, V.H., Jaenisch,
910 R., Corr, M., Nizet, V.*, et al.* (2003). HIF-1alpha is essential for myeloid cell-mediated inflammation. Cell
911 *112*, 645-657.
912
913 Danet, G.H., Pan, Y., Luongo, J.L., Bonnet, D.A., and Simon, M.C. (2003). Expansion of human SCID-
914 repopulating cells under hypoxic conditions. J Clin Invest *112*, 126-135.
915
916 Dang, E.V., Barbi, J., Yang, H.Y., Jinasena, D., Yu, H., Zheng, Y., Bordman, Z., Fu, J., Kim, Y., Yen,
917 H.R.*, et al.* (2011). Control of T(H)17/T(reg) balance by hypoxia-inducible factor 1. Cell *146*, 772-784.
918
919 de Almeida, M.J., Luchsinger, L.L., Corrigan, D.J., Williams, L.J., and Snoeck, H.W. (2017). Dye-
920 Independent Methods Reveal Elevated Mitochondrial Mass in Hematopoietic Stem Cells. Cell Stem Cell
921 *21*, 725-729 e724.
922
923 Ding, L., and Morrison, S.J. (2013). Haematopoietic stem cells and early lymphoid progenitors occupy
924 distinct bone marrow niches. Nature *495*, 231-235.
925
926 Doedens, A.L., Phan, A.T., Stradner, M.H., Fujimoto, J.K., Nguyen, J.V., Yang, E., Johnson, R.S., and
927 Goldrath, A.W. (2013). Hypoxia-inducible factors enhance the effector responses of CD8(+) T cells to
928 persistent antigen. Nat Immunol *14*, 1173-1182.
929
930 Doulatov, S., Notta, F., Eppert, K., Nguyen, L.T., Ohashi, P.S., and Dick, J.E. (2010). Revised map of the
931 human progenitor hierarchy shows the origin of macrophages and dendritic cells in early lymphoid
932 development. Nat Immunol *11*, 585-593.
933
934 Doulatov, S., Notta, F., Laurenti, E., and Dick, J.E. (2012). Hematopoiesis: a human perspective. Cell
935 Stem Cell *10*, 120-136.
936
937 Eliasson, P., and Jonsson, J.I. (2010). The hematopoietic stem cell niche: low in oxygen but a nice place to
938 be. J Cell Physiol *222*, 17-22.
939
940 Fang, H.Y., Hughes, R., Murdoch, C., Coffelt, S.B., Biswas, S.K., Harris, A.L., Johnson, R.S., Imityaz,
941 H.Z., Simon, M.C., Fredlund, E.*, et al.* (2009). Hypoxia-inducible factors 1 and 2 are important
942 transcriptional effectors in primary macrophages experiencing hypoxia. Blood *114*, 844-859.
943
944 Felices, M., Ankarlo, D.E., Lenvik, T.R., Nelson, H.H., Blazar, B.R., Verneris, M.R., and Miller, J.S.
945 (2014). Notch signaling at later stages of NK cell development enhances KIR expression and functional
946 maturation. J Immunol *193*, 3344-3354.
947

948 Forristal, C.E., Nowlan, B., Jacobsen, R.N., Barbier, V., Walkinshaw, G., Walkley, C.R., Winkler, I.G.,
949 and Levesque, J.P. (2015). HIF-1alpha is required for hematopoietic stem cell mobilization and 4-prolyl
950 hydroxylase inhibitors enhance mobilization by stabilizing HIF-1alpha. Leukemia *29*, 1366-1378.
951
952 Galy, A., Travis, M., Cen, D., and Chen, B. (1995). Human T, B, natural killer, and dendritic cells arise
953 from a common bone marrow progenitor cell subset. Immunity *3*, 459-473.
954
955 Goardon, N., Marchi, E., Atzberger, A., Quek, L., Schuh, A., Soneji, S., Woll, P., Mead, A., Alford, K.A.,
956 Rout, R.*, et al.* (2011). Coexistence of LMPP-like and GMP-like leukemia stem cells in acute myeloid
957 leukemia. Cancer Cell *19*, 138-152.
958
959 Gomez-Puerto, M.C., Folkerts, H., Wierenga, A.T., Schepers, K., Schuringa, J.J., Coffer, P.J., and
960 Vellenga, E. (2016). Autophagy Proteins ATG5 and ATG7 Are Essential for the Maintenance of Human
961 CD34(+) Hematopoietic Stem-Progenitor Cells. Stem Cells *34*, 1651-1663.
962
963 Guitart, A.V., Hammoud, M., Dello Sbarba, P., Ivanovic, Z., and Praloran, V. (2010). Slow-
964 cycling/quiescence balance of hematopoietic stem cells is related to physiological gradient of oxygen. Exp
965 Hematol *38*, 847-851.
966
967 Guitart, A.V., Subramani, C., Armesilla-Diaz, A., Smith, G., Sepulveda, C., Gezer, D., Vukovic, M.,
968 Dunn, K., Pollard, P., Holyoake, T.L.*, et al.* (2013). Hif-2alpha is not essential for cell-autonomous
969 hematopoietic stem cell maintenance. Blood *122*, 1741-1745.
970
971 Haddad, R., Guardiola, P., Izac, B., Thibault, C., Radich, J., Delezoide, A.L., Baillou, C., Lemoine, F.M.,
972 Gluckman, J.C., Pflumio, F.*, et al.* (2004). Molecular characterization of early human T/NK and B-
973 lymphoid progenitor cells in umbilical cord blood. Blood *104*, 3918-3926.
974
975 Haddad, R., Guimiot, F., Six, E., Jourquin, F., Setterblad, N., Kahn, E., Yagello, M., Schiffer, C., Andre-
976 Schmutz, I., Cavazzana-Calvo, M.*, et al.* (2006). Dynamics of thymus-colonizing cells during human
977 development. Immunity *24*, 217-230.
978
979 Haddad, R., Pflumio, F., Vigon, I., Visentin, G., Auvray, C., Fichelson, S., and Amsellem, S. (2008). The
980 HOXB4 homeoprotein differentially promotes ex vivo expansion of early human lymphoid progenitors.
981 Stem Cells *26*, 312-322.
982
983 Hale, L.P., Braun, R.D., Gwinn, W.M., Greer, P.K., and Dewhirst, M.W. (2002). Hypoxia in the thymus:
984 role of oxygen tension in thymocyte survival. Am J Physiol Heart Circ Physiol *282*, H1467-1477.
985
986 Halvarsson, C., Eliasson, P., and Jonsson, J.I. (2017). Pyruvate dehydrogenase kinase 1 is essential for
987 transplantable mouse bone marrow hematopoietic stem cell and progenitor function. PLoS One *12*,
988 e0171714.
989
990 Hammoud, M., Vlaski, M., Duchez, P., Chevaleyre, J., Lafarge, X., Boiron, J.M., Praloran, V., Brunet De
991 La Grange, P., and Ivanovic, Z. (2012). Combination of low O(2) concentration and mesenchymal stromal
992 cells during culture of cord blood CD34(+) cells improves the maintenance and proliferative capacity of
993 hematopoietic stem cells. J Cell Physiol *227*, 2750-2758.
994
995 Hao, Q.L., Smogorzewska, E.M., Barsky, L.W., and Crooks, G.M. (1998). In vitro identification of single
996 CD34+CD38- cells with both lymphoid and myeloid potential. Blood *91*, 4145-4151.
997

Hermitte, F., Brunet de la Grange, P., Belloc, F., Praloran, V., and Ivanovic, Z. (2006). Very low O2 concentration (0.1%) favors G0 return of dividing CD34+ cells. Stem Cells *24*, 65-73.

Ho, T.T., Warr, M.R., Adelman, E.R., Lansinger, O.M., Flach, J., Verovskaya, E.V., Figueroa, M.E., and Passegue, E. (2017). Autophagy maintains the metabolism and function of young and old stem cells. Nature *543*, 205-210.

Ianniciello, A., Dumas, P.Y., Drullion, C., Guitart, A., Villacreces, A., Peytour, Y., Chevaleyre, J., Brunet de la Grange, P., Vigon, I., Desplat, V.*, et al.* (2017). Chronic myeloid leukemia progenitor cells require autophagy when leaving hypoxia-induced quiescence. Oncotarget *8*, 96984-96992.

Imanirad, P., Solaimani Kartalaei, P., Crisan, M., Vink, C., Yamada-Inagawa, T., de Pater, E., Kurek, D., Kaimakis, P., van der Linden, R., Speck, N.*, et al.* (2014). HIF1alpha is a regulator of hematopoietic progenitor and stem cell development in hypoxic sites of the mouse embryo. Stem Cell Res *12*, 24-35.

Ivanovic, Z., Dello Sbarba, P., Trimoreau, F., Faucher, J.L., and Praloran, V. (2000). Primitive human HPCs are better maintained and expanded in vitro at 1 percent oxygen than at 20 percent. Transfusion *40*, 1482-1488.

Ivanovic, Z., Hermitte, F., Brunet de la Grange, P., Dazey, B., Belloc, F., Lacombe, F., Vezon, G., and Praloran, V. (2004). Simultaneous maintenance of human cord blood SCID-repopulating cells and expansion of committed progenitors at low O2 concentration (3%). Stem Cells *22*, 716-724.

Joshi, S., Singh, A.R., Zulcic, M., and Durden, D.L. (2014). A macrophage-dominant PI3K isoform controls hypoxia-induced HIF1alpha and HIF2alpha stability and tumor growth, angiogenesis, and metastasis. Mol Cancer Res *12*, 1520-1531.

Karamitros, D., Stoilova, B., Aboukhalil, Z., Hamey, F., Reinisch, A., Samitsch, M., Quek, L., Otto, G., Repapi, E., Doondeea, J.*, et al.* (2018). Single-cell analysis reveals the continuum of human lympho-myeloid progenitor cells. Nat Immunol *19*, 85-97.

Kohn, L.A., Hao, Q.L., Sasidharan, R., Parekh, C., Ge, S., Zhu, Y., Mikkola, H.K., and Crooks, G.M. (2012). Lymphoid priming in human bone marrow begins before expression of CD10 with upregulation of L-selectin. Nat Immunol *13*, 963-971.

Kojima, H., Gu, H., Nomura, S., Caldwell, C.C., Kobata, T., Carmeliet, P., Semenza, G.L., and Sitkovsky, M.V. (2002). Abnormal B lymphocyte development and autoimmunity in hypoxia-inducible factor 1alpha -deficient chimeric mice. Proc Natl Acad Sci U S A *99*, 2170-2174.

Kojima, H., Kobayashi, A., Sakurai, D., Kanno, Y., Hase, H., Takahashi, R., Totsuka, Y., Semenza, G.L., Sitkovsky, M.V., and Kobata, T. (2010). Differentiation stage-specific requirement in hypoxia-inducible factor-1alpha-regulated glycolytic pathway during murine B cell development in bone marrow. J Immunol *184*, 154-163.

Koller, M.R., Bender, J.G., Miller, W.M., and Papoutsakis, E.T. (1992). Reduced oxygen tension increases hematopoiesis in long-term culture of human stem and progenitor cells from cord blood and bone marrow. Exp Hematol *20*, 264-270.

Krock, B.L., Eisinger-Mathason, T.S., Giannoukos, D.N., Shay, J.E., Gohil, M., Lee, D.S., Nakazawa, M.S., Sesen, J., Skuli, N., and Simon, M.C. (2015). The aryl hydrocarbon receptor nuclear translocator is an essential regulator of murine hematopoietic stem cell viability. Blood *125*, 3263-3272.

Krzywinska, E., Kantari-Mimoun, C., Kerdiles, Y., Sobecki, M., Isagawa, T., Gotthardt, D., Castells, M., Haubold, J., Millien, C., Viel, T.*, et al.* (2017). Loss of HIF-1alpha in natural killer cells inhibits tumour growth by stimulating non-productive angiogenesis. Nat Commun *8*, 1597.

Kuang, R., Jahangiri, A., Mascharak, S., Nguyen, A., Chandra, A., Flanigan, P.M., Yagnik, G., Wagner, J.R., De Lay, M., Carrera, D.*, et al.* (2017). GLUT3 upregulation promotes metabolic reprogramming associated with antiangiogenic therapy resistance. JCI Insight *2*, e88815.

Kubota, Y., Takubo, K., and Suda, T. (2008). Bone marrow long label-retaining cells reside in the sinusoidal hypoxic niche. Biochem Biophys Res Commun *366*, 335-339.

Larbi, A., Mitjavila-Garcia, M.T., Flamant, S., Valogne, Y., Clay, D., Usunier, B., l'Homme, B., Feraud, O., Casal, I., Gobbo, E.*, et al.* (2014). Generation of multipotent early lymphoid progenitors from human embryonic stem cells. Stem Cells Dev *23*, 2983-2995.

Laurenti, E., Doulatov, S., Zandi, S., Plumb, I., Chen, J., April, C., Fan, J.B., and Dick, J.E. (2013). The transcriptional architecture of early human hematopoiesis identifies multilevel control of lymphoid commitment. Nat Immunol *14*, 756-763.

Levesque, J.P., Winkler, I.G., Hendy, J., Williams, B., Helwani, F., Barbier, V., Nowlan, B., and Nilsson, S.K. (2007). Hematopoietic progenitor cell mobilization results in hypoxia with increased hypoxia-inducible transcription factor-1 alpha and vascular endothelial growth factor A in bone marrow. Stem Cells *25*, 1954-1965.

Majeti, R., Park, C.Y., and Weissman, I.L. (2007). Identification of a hierarchy of multipotent hematopoietic progenitors in human cord blood. Cell Stem Cell *1*, 635-645.

Majmundar, A.J., Wong, W.J., and Simon, M.C. (2010). Hypoxia-inducible factors and the response to hypoxic stress. Mol Cell *40*, 294-309.

Mantel, C.R., O'Leary, H.A., Chitteti, B.R., Huang, X., Cooper, S., Hangoc, G., Brustovetsky, N., Srour, E.F., Lee, M.R., Messina-Graham, S.*, et al.* (2015). Enhancing Hematopoietic Stem Cell Transplantation Efficacy by Mitigating Oxygen Shock. Cell *161*, 1553-1565.

Mazurier, F., Doedens, M., Gan, O.I., and Dick, J.E. (2003). Rapid myeloerythroid repopulation after intrafemoral transplantation of NOD-SCID mice reveals a new class of human stem cells. Nat Med *9*, 959-963.

McNamee, E.N., Korns Johnson, D., Homann, D., and Clambey, E.T. (2013). Hypoxia and hypoxia-inducible factors as regulators of T cell development, differentiation, and function. Immunol Res *55*, 58-70.

Mendelson, A., and Frenette, P.S. (2014). Hematopoietic stem cell niche maintenance during homeostasis and regeneration. Nat Med *20*, 833-846.

Meng, X., Grotsch, B., Luo, Y., Knaup, K.X., Wiesener, M.S., Chen, X.X., Jantsch, J., Fillatreau, S., Schett, G., and Bozec, A. (2018). Hypoxia-inducible factor-1alpha is a critical transcription factor for IL-10-producing B cells in autoimmune disease. Nat Commun *9*, 251.

Mohyeldin, A., Garzon-Muvdi, T., and Quinones-Hinojosa, A. (2010). Oxygen in stem cell biology: a critical component of the stem cell niche. Cell Stem Cell *7*, 150-161.

Morrison, S.J., and Scadden, D.T. (2014). The bone marrow niche for haematopoietic stem cells. Nature *505*, 327-334.

Nombela-Arrieta, C., Pivarnik, G., Winkel, B., Canty, K.J., Harley, B., Mahoney, J.E., Park, S.Y., Lu, J., Protopopov, A., and Silberstein, L.E. (2013). Quantitative imaging of haematopoietic stem and progenitor cell localization and hypoxic status in the bone marrow microenvironment. Nat Cell Biol *15*, 533-543.

Notta, F., Zandi, S., Takayama, N., Dobson, S., Gan, O.I., Wilson, G., Kaufmann, K.B., McLeod, J., Laurenti, E., Dunant, C.F., *et al.* (2016). Distinct routes of lineage development reshape the human blood hierarchy across ontogeny. Science *351*, aab2116.

O'Riordan, M., and Grosschedl, R. (1999). Coordinate regulation of B cell differentiation by the transcription factors EBF and E2A. Immunity *11*, 21-31.

Ohta, A., Diwanji, R., Kini, R., Subramanian, M., Ohta, A., and Sitkovsky, M. (2011). In vivo T cell activation in lymphoid tissues is inhibited in the oxygen-poor microenvironment. Front Immunol *2*, 27.

Palazon, A., Tyrakis, P.A., Macias, D., Velica, P., Rundqvist, H., Fitzpatrick, S., Vojnovic, N., Phan, A.T., Loman, N., Hedenfalk, I., *et al.* (2017). An HIF-1alpha/VEGF-A Axis in Cytotoxic T Cells Regulates Tumor Progression. Cancer Cell *32*, 669-683 e665.

Parmar, K., Mauch, P., Vergilio, J.A., Sackstein, R., and Down, J.D. (2007). Distribution of hematopoietic stem cells in the bone marrow according to regional hypoxia. Proc Natl Acad Sci U S A *104*, 5431-5436.

Renoux, V.M., Zriwil, A., Peitzsch, C., Michaelsson, J., Friberg, D., Soneji, S., and Sitnicka, E. (2015). Identification of a Human Natural Killer Cell Lineage-Restricted Progenitor in Fetal and Adult Tissues. Immunity *43*, 394-407.

Robin, C., Pflumio, F., Vainchenker, W., and Coulombel, L. (1999). Identification of lymphomyeloid primitive progenitor cells in fresh human cord blood and in the marrow of nonobese diabetic-severe combined immunodeficient (NOD-SCID) mice transplanted with human CD34(+) cord blood cells. J Exp Med *189*, 1601-1610.

Rouault-Pierre, K., Lopez-Onieva, L., Foster, K., Anjos-Afonso, F., Lamrissi-Garcia, I., Serrano-Sanchez, M., Mitter, R., Ivanovic, Z., de Verneuil, H., Gribben, J., *et al.* (2013). HIF-2alpha protects human hematopoietic stem/progenitors and acute myeloid leukemic cells from apoptosis induced by endoplasmic reticulum stress. Cell Stem Cell *13*, 549-563.

Schilham, M.W., Moerer, P., Cumano, A., and Clevers, H.C. (1997). Sox-4 facilitates thymocyte differentiation. Eur J Immunol *27*, 1292-1295.

Schilham, M.W., Oosterwegel, M.A., Moerer, P., Ya, J., de Boer, P.A., van de Wetering, M., Verbeek, S., Lamers, W.H., Kruisbeek, A.M., Cumano, A., *et al.* (1996). Defects in cardiac outflow tract formation and pro-B-lymphocyte expansion in mice lacking Sox-4. Nature *380*, 711-714.

Semenza, G.L. (2012). Hypoxia-inducible factors in physiology and medicine. Cell *148*, 399-408.

Shima, H., Takubo, K., Iwasaki, H., Yoshihara, H., Gomei, Y., Hosokawa, K., Arai, F., Takahashi, T., and Suda, T. (2009). Reconstitution activity of hypoxic cultured human cord blood CD34-positive cells in NOG mice. Biochem Biophys Res Commun *378*, 467-472.

Shima, H., Takubo, K., Tago, N., Iwasaki, H., Arai, F., Takahashi, T., and Suda, T. (2010). Acquisition of G(0) state by CD34-positive cord blood cells after bone marrow transplantation. Exp Hematol *38*, 1231-1240.

Simsek, T., Kocabas, F., Zheng, J., Deberardinis, R.J., Mahmoud, A.I., Olson, E.N., Schneider, J.W., Zhang, C.C., and Sadek, H.A. (2010). The distinct metabolic profile of hematopoietic stem cells reflects their location in a hypoxic niche. Cell Stem Cell *7*, 380-390.

Sirven, A., Pflumio, F., Zennou, V., Titeux, M., Vainchenker, W., Coulombel, L., Dubart-Kupperschmitt, A., and Charneau, P. (2000). The human immunodeficiency virus type-1 central DNA flap is a crucial determinant for lentiviral vector nuclear import and gene transduction of human hematopoietic stem cells. Blood *96*, 4103-4110.

Six, E.M., Bonhomme, D., Monteiro, M., Beldjord, K., Jurkowska, M., Cordier-Garcia, C., Garrigue, A., Dal Cortivo, L., Rocha, B., Fischer, A.*, et al.* (2007). A human postnatal lymphoid progenitor capable of circulating and seeding the thymus. J Exp Med *204*, 3085-3093.

Spencer, J.A., Ferraro, F., Roussakis, E., Klein, A., Wu, J., Runnels, J.M., Zaher, W., Mortensen, L.J., Alt, C., Turcotte, R.*, et al.* (2014). Direct measurement of local oxygen concentration in the bone marrow of live animals. Nature *508*, 269-273.

Suda, T., Takubo, K., and Semenza, G.L. (2011). Metabolic regulation of hematopoietic stem cells in the hypoxic niche. Cell Stem Cell *9*, 298-310.

Takubo, K., Goda, N., Yamada, W., Iriuchishima, H., Ikeda, E., Kubota, Y., Shima, H., Johnson, R.S., Hirao, A., Suematsu, M.*, et al.* (2010). Regulation of the HIF-1alpha level is essential for hematopoietic stem cells. Cell Stem Cell *7*, 391-402.

Testa, U., Labbaye, C., Castelli, G., and Pelosi, E. (2016). Oxidative stress and hypoxia in normal and leukemic stem cells. Exp Hematol *44*, 540-560.

Tsuboi, I., Yamashita, T., Nagano, M., Kimura, K., To'a Salazar, G., and Ohneda, O. (2015). Impaired expression of HIF-2alpha induces compensatory expression of HIF-1alpha for the recovery from anemia. J Cell Physiol *230*, 1534-1548.

Vong, Q.P., Leung, W.H., Houston, J., Li, Y., Rooney, B., Holladay, M., Oostendorp, R.A., and Leung, W. (2014). TOX2 regulates human natural killer cell development by controlling T-BET expression. Blood *124*, 3905-3913.

Vukovic, M., Sepulveda, C., Subramani, C., Guitart, A.V., Mohr, J., Allen, L., Panagopoulou, T.I., Paris, J., Lawson, H., Villacreces, A.*, et al.* (2016). Adult hematopoietic stem cells lacking Hif-1alpha self-renew normally. Blood *127*, 2841-2846.

Wang, S., He, Q., Ma, D., Xue, Y., and Liu, F. (2015). Irf4 Regulates the Choice between T Lymphoid-Primed Progenitor and Myeloid Lineage Fates during Embryogenesis. Dev Cell *34*, 621-631.

Warr, M.R., Binnewies, M., Flach, J., Reynaud, D., Garg, T., Malhotra, R., Debnath, J., and Passegue, E. (2013). FOXO3A directs a protective autophagy program in haematopoietic stem cells. Nature *494*, 323-327.

Xu, Y., Chaudhury, A., Zhang, M., Savoldo, B., Metelitsa, L.S., Rodgers, J., Yustein, J.T., Neilson, J.R., and Dotti, G. (2016). Glycolysis determines dichotomous regulation of T cell subsets in hypoxia. J Clin Invest *126*, 2678-2688.

Yu, J., Freud, A.G., and Caligiuri, M.A. (2013). Location and cellular stages of natural killer cell development. Trends Immunol *34*, 573-582.

Yun, S., Lee, S.H., Yoon, S.R., Myung, P.K., and Choi, I. (2011). Oxygen tension regulates NK cells differentiation from hematopoietic stem cells in vitro. Immunol Lett *137*, 70-77.

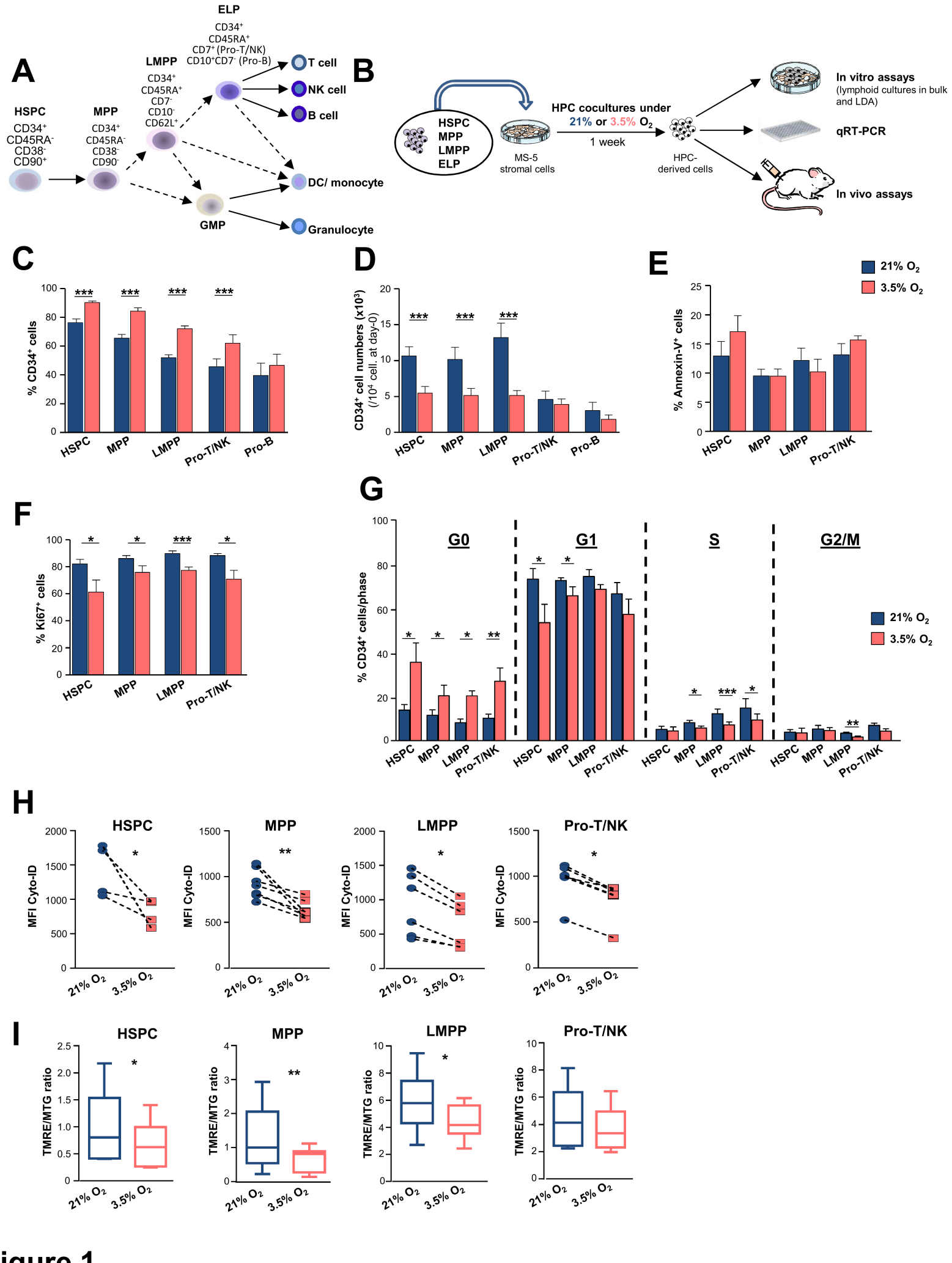
A
HSPC
CD34+ CD45RA- CD38- CD90+
MPP
CD34+ CD45RA- CD38- CD90-
LMPP
CD34+ CD45RA+ CD7- CD10- CD62L+
ELP
CD34+ CD45RA+ CD7+ (Pro-T/NK) CD10+CD7- (Pro-B)
GMP
T cell
NK cell
B cell
DC/ monocyte
Granulocyte
B
HSPC MPP LMPP ELP
MS-5 stromal cells
HPC cocultures under 21% or 3.5% O2
1 week
HPC-derived cells
In vitro assays (lymphoid cultures in bulk and LDA)
qRT-PCR
In vivo assays
C
% CD34+ cells
HSPC MPP LMPP Pro-T/NK Pro-B
D
CD34+ cell numbers (x10³) (/10⁴ cell. at day-0)
HSPC MPP LMPP Pro-T/NK Pro-B
E
21% O2
3.5% O2
% Annexin-V+ cells
HSPC MPP LMPP Pro-T/NK
F
% Ki67+ cells
HSPC MPP LMPP Pro-T/NK
G
% CD34+ cells/phase
G0 G1 S G2/M
21% O2
3.5% O2
HSPC MPP LMPP Pro-T/NK
H
HSPC MPP LMPP Pro-T/NK
MFI Cyto-ID
21% O2 3.5% O2
I
HSPC MPP LMPP Pro-T/NK
TMRE/MTG ratio
21% O2 3.5% O2

Figure 1

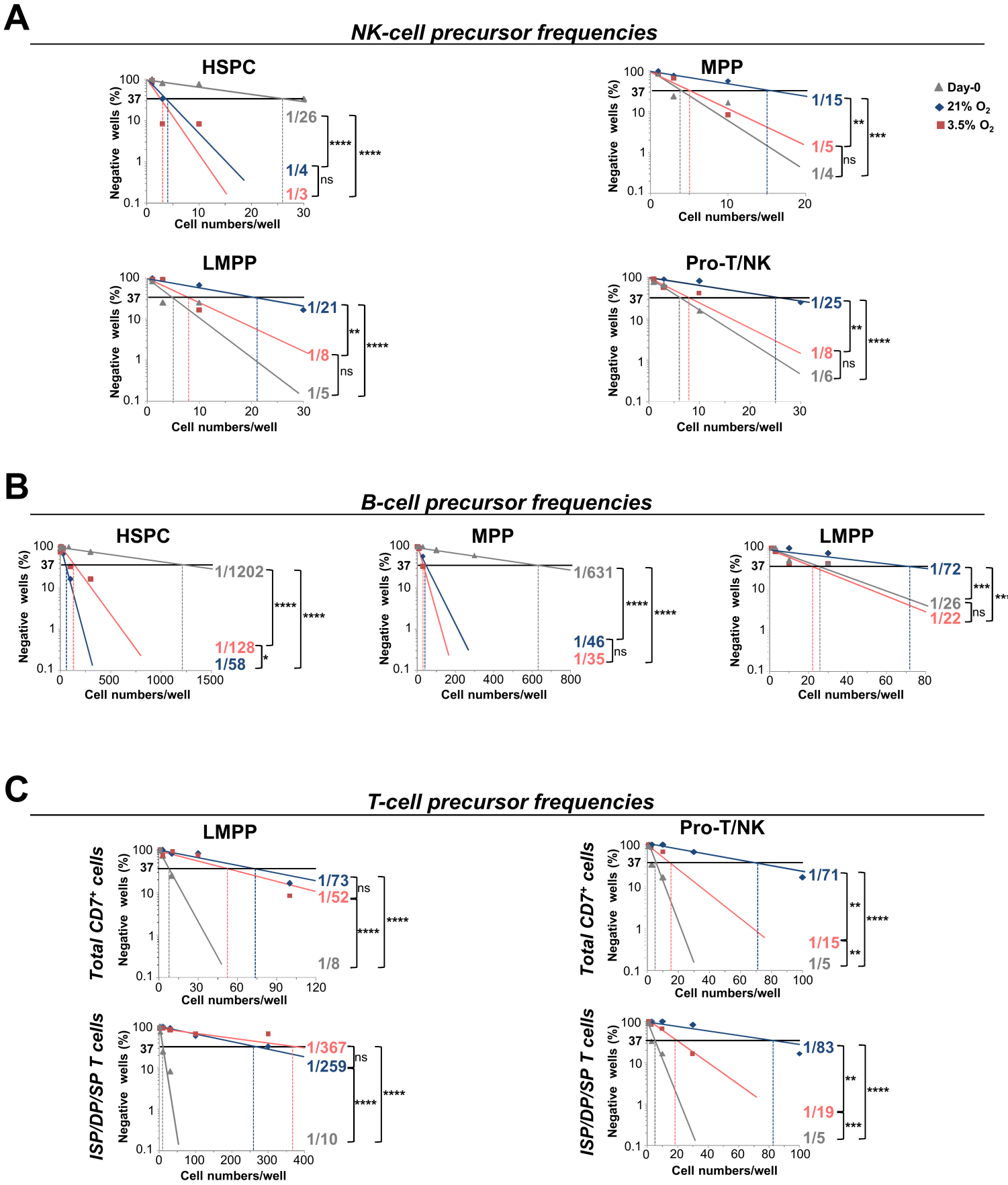
A
NK-cell precursor frequencies
HSPC
MPP
LMPP
Pro-T/NK
Day-0
21% O2
3.5% O2
Negative wells (%)
Cell numbers/well
1/26
1/4
1/3
1/15
1/5
1/4
1/21
1/8
1/5
1/25
1/8
1/6
B
B-cell precursor frequencies
HSPC
MPP
LMPP
1/1202
1/128
1/58
1/631
1/46
1/35
1/72
1/26
1/22
C
T-cell precursor frequencies
LMPP
Pro-T/NK
Total CD7+ cells
ISP/DP/SP T cells
1/73
1/52
1/8
1/71
1/15
1/5
1/367
1/259
1/10
1/83
1/19
1/5

Figure 2

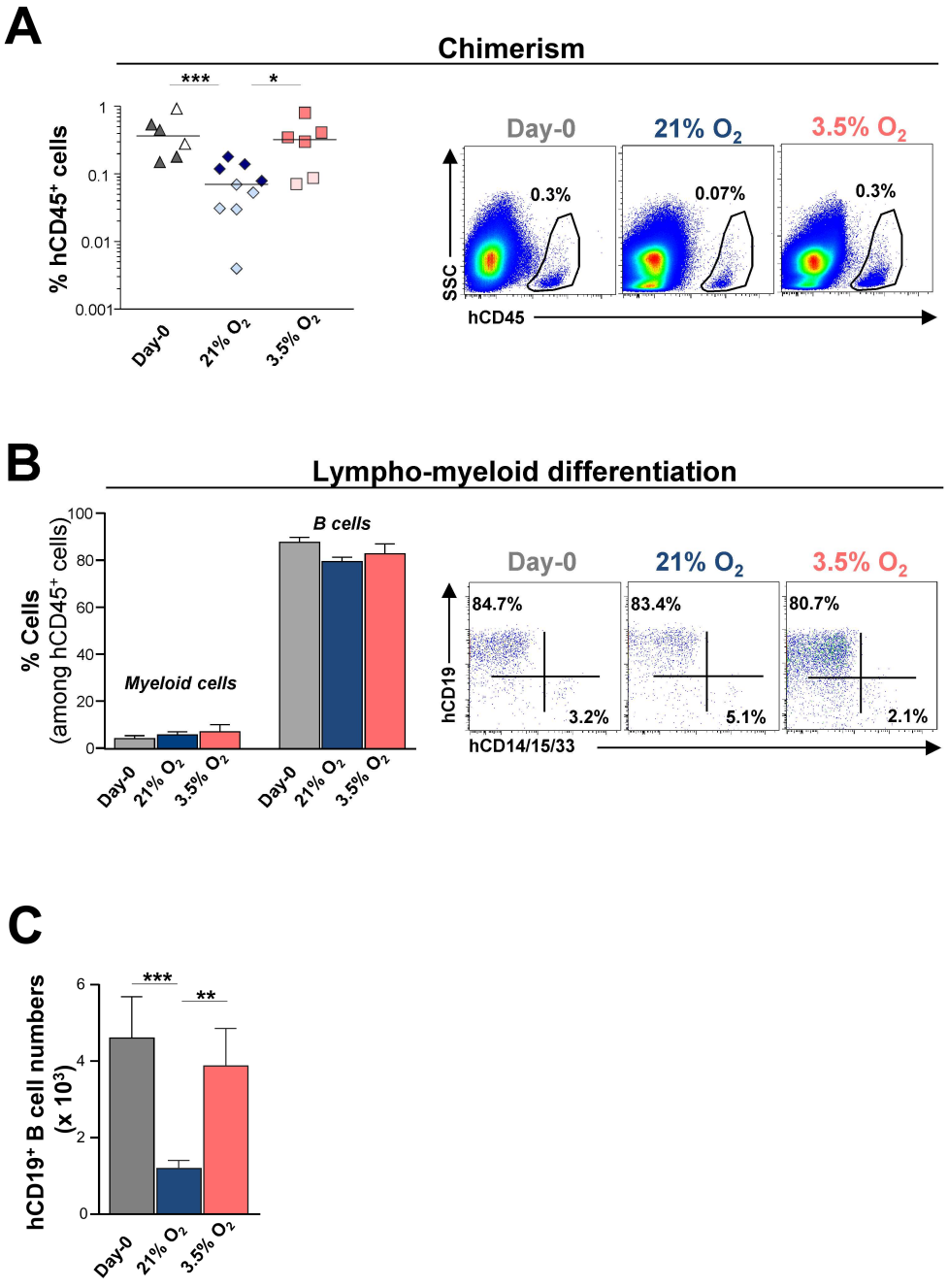
A
Chimerism
***
*
% hCD45+ cells
1
0.1
0.01
0.001
Day-0
21% O2
3.5% O2
Day-0
21% O2
3.5% O2
0.3%
0.07%
0.3%
SSC
hCD45
B
Lympho-myeloid differentiation
% Cells
(among hCD45+ cells)
100
80
60
40
20
0
B cells
Myeloid cells
Day-0
21% O2
3.5% O2
Day-0
21% O2
3.5% O2
Day-0
21% O2
3.5% O2
84.7%
83.4%
80.7%
3.2%
5.1%
2.1%
hCD19
hCD14/15/33
C
***
**
hCD19+ B cell numbers
(x 10³)
6
4
2
0
Day-0
21% O2
3.5% O2

Figure 3

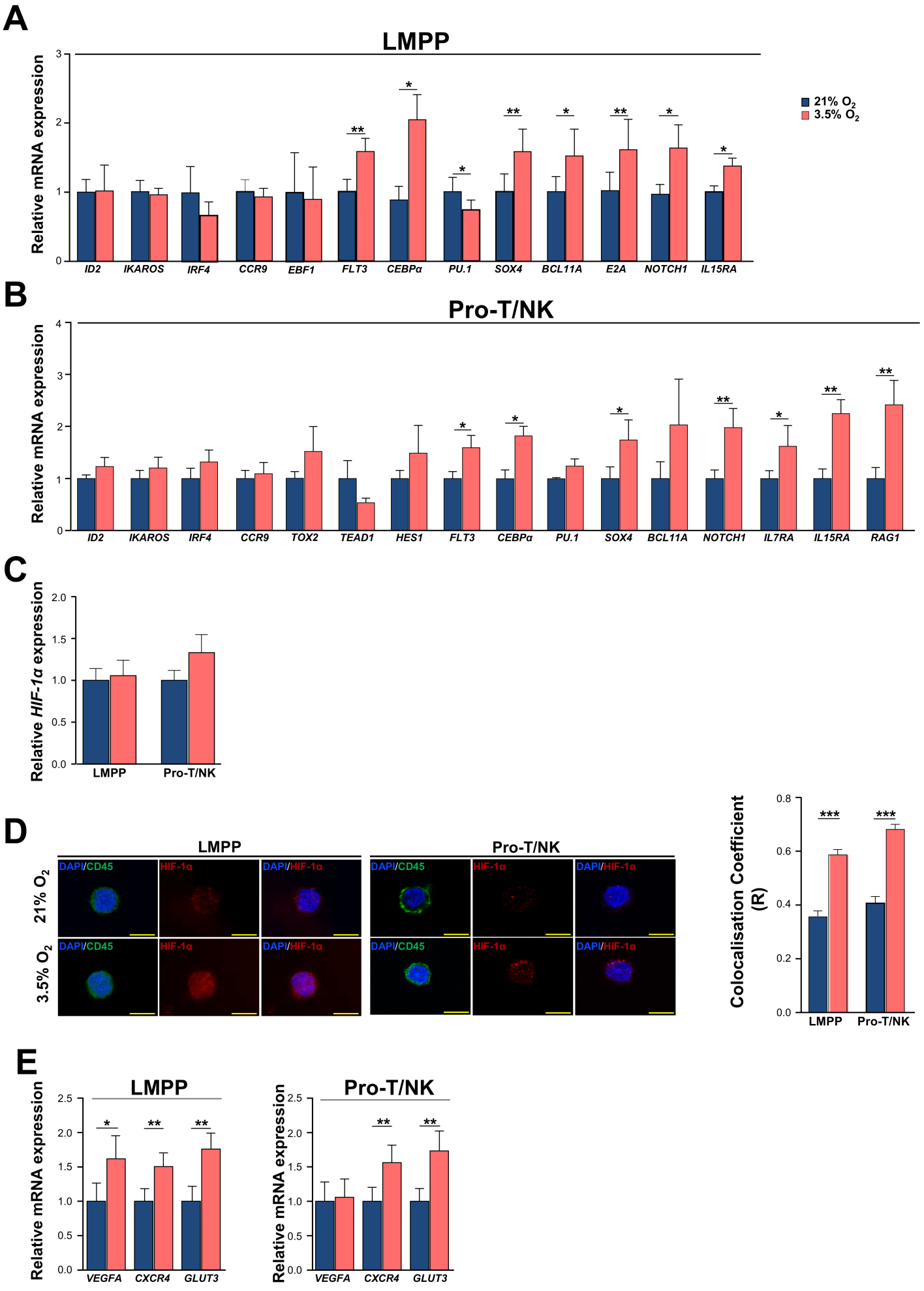
A
LMPP
Relative mRNA expression
21% O2
3.5% O2
ID2
IKAROS
IRF4
CCR9
EBF1
FLT3
CEBPα
PU.1
SOX4
BCL11A
E2A
NOTCH1
IL15RA
B
Pro-T/NK
Relative mRNA expression
ID2
IKAROS
IRF4
CCR9
TOX2
TEAD1
HES1
FLT3
CEBPα
PU.1
SOX4
BCL11A
NOTCH1
IL7RA
IL15RA
RAG1
C
Relative HIF-1α expression
LMPP
Pro-T/NK
D
LMPP
Pro-T/NK
21% O2
3.5% O2
DAPI/CD45
HIF-1α
DAPI/HIF-1α
Colocalisation Coefficient (R)
LMPP
Pro-T/NK
E
LMPP
Pro-T/NK
Relative mRNA expression
VEGFA
CXCR4
GLUT3

Figure 4

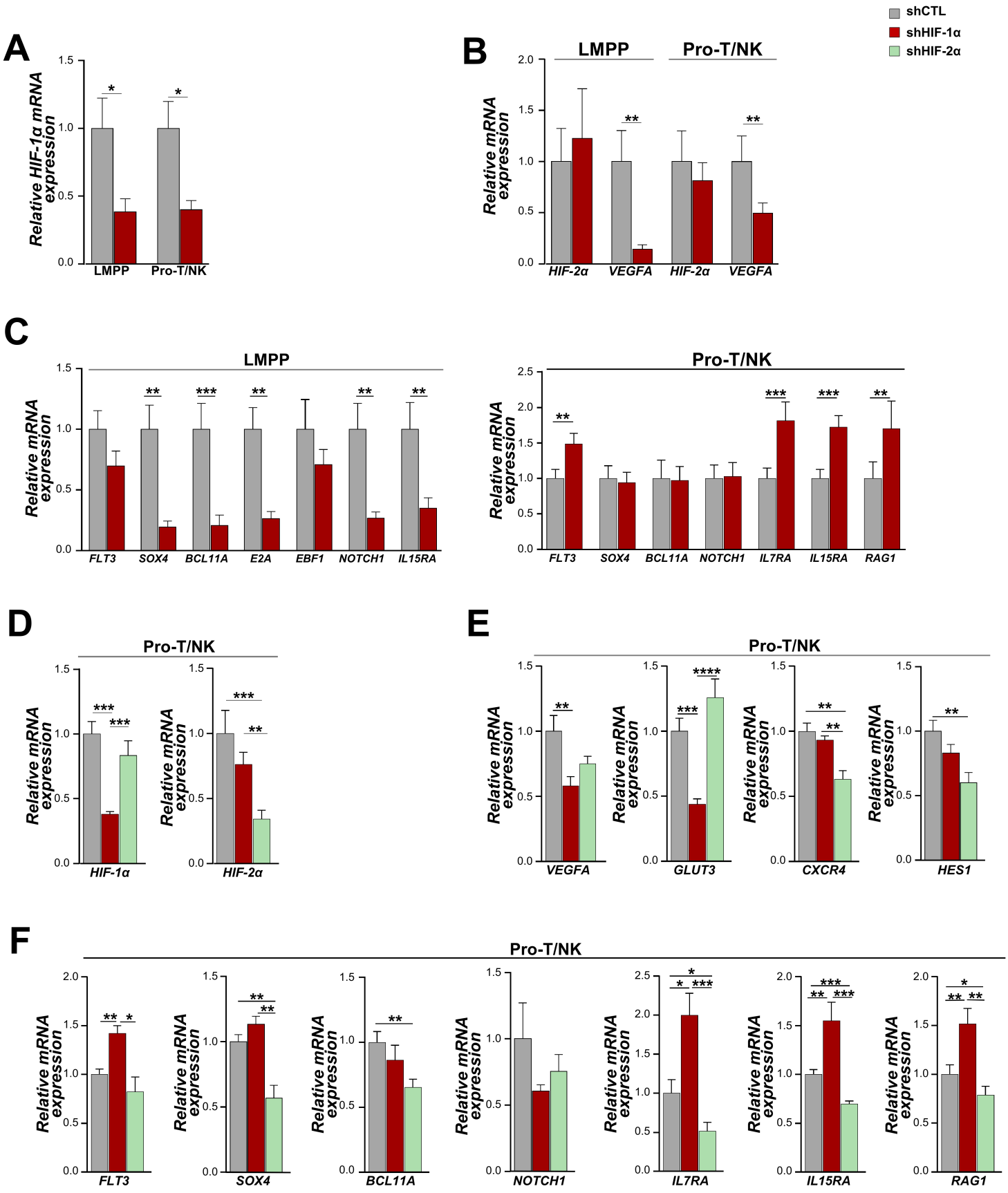
A
Relative HIF-1α mRNA expression
LMPP
Pro-T/NK
B
shCTL
shHIF-1α
shHIF-2α
LMPP
Pro-T/NK
Relative mRNA expression
HIF-2α
VEGFA
HIF-2α
VEGFA
C
LMPP
Relative mRNA expression
FLT3
SOX4
BCL11A
E2A
EBF1
NOTCH1
IL15RA
Pro-T/NK
FLT3
SOX4
BCL11A
NOTCH1
IL7RA
IL15RA
RAG1
D
Pro-T/NK
HIF-1α
HIF-2α
E
Pro-T/NK
VEGFA
GLUT3
CXCR4
HES1
F
Pro-T/NK
FLT3
SOX4
BCL11A
NOTCH1
IL7RA
IL15RA
RAG1

Figure 5

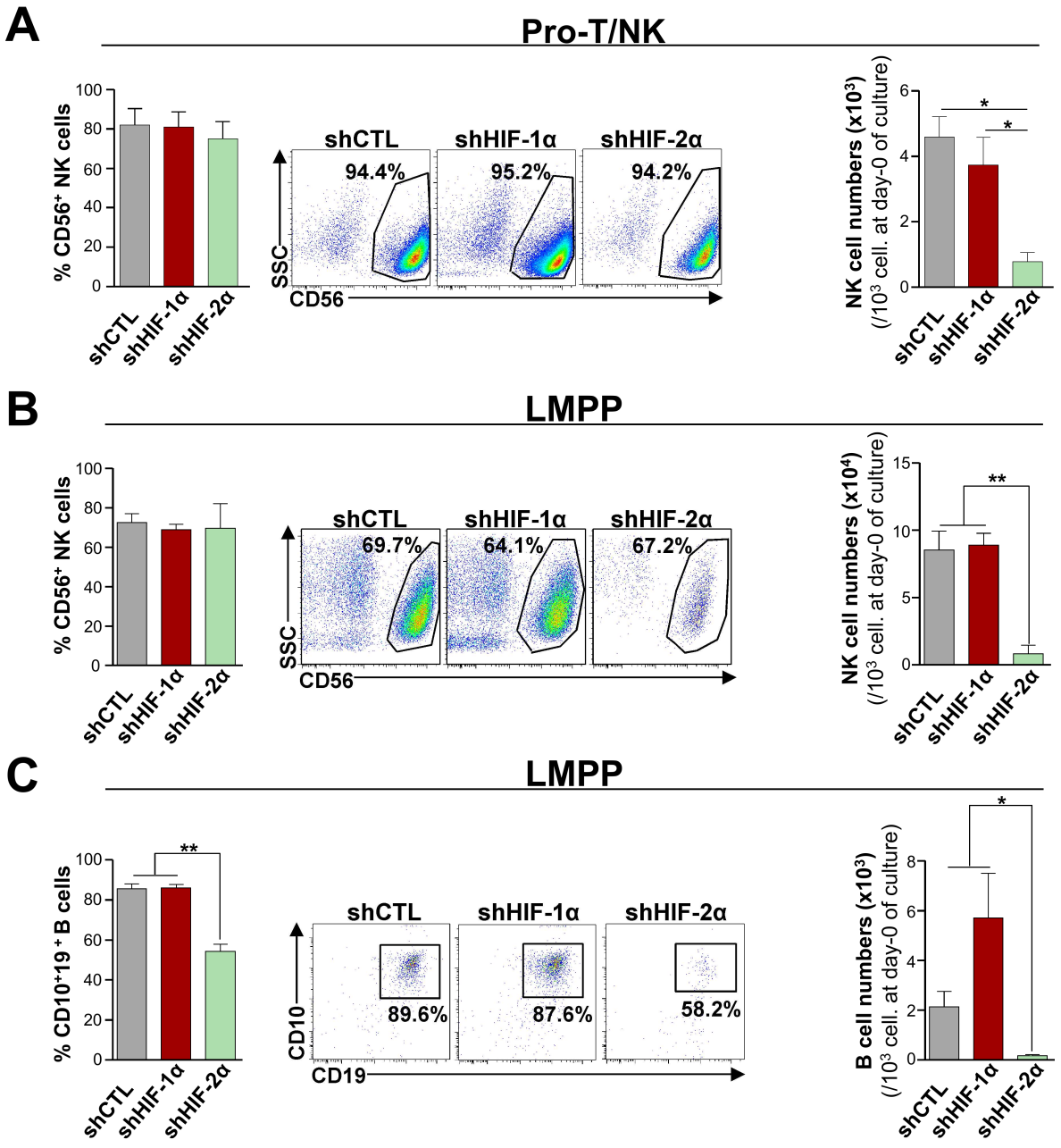
A
Pro-T/NK
% CD56+ NK cells
shCTL
shHIF-1α
shHIF-2α
94.4%
95.2%
94.2%
SSC
CD56
NK cell numbers (x10³)
(/10³ cell. at day-0 of culture)
B
LMPP
% CD56+ NK cells
69.7%
64.1%
67.2%
NK cell numbers (x10⁴)
(/10³ cell. at day-0 of culture)
C
LMPP
% CD10+19+ B cells
89.6%
87.6%
58.2%
CD10
CD19
B cell numbers (x10³)
(/10³ cell. at day-0 of culture)

Figure 6

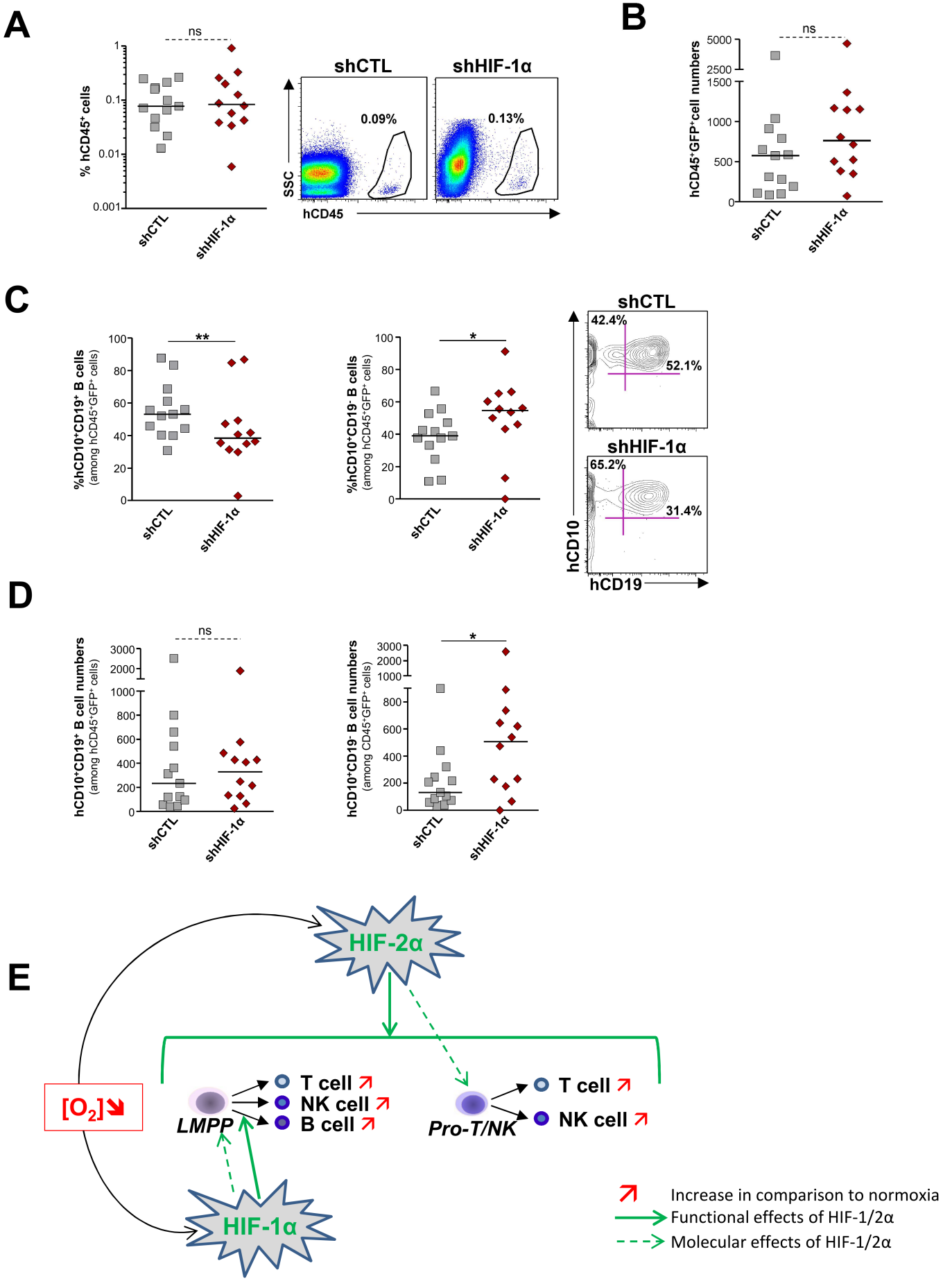
A
ns
% hCD45+ cells
shCTL
shHIF-1α
shCTL
shHIF-1α
0.09%
0.13%
SSC
hCD45
B
ns
hCD45+GFP+cell numbers
shCTL
shHIF-1α
C
**
%hCD10+CD19+ B cells
(among hCD45+GFP+ cells)
shCTL
shHIF-1α
*
%hCD10+CD19- B cells
(among hCD45+GFP+ cells)
shCTL
shHIF-1α
shCTL
42.4%
52.1%
shHIF-1α
65.2%
31.4%
hCD10
hCD19
D
ns
hCD10+CD19+ B cell numbers
(among hCD45+GFP+ cells)
shCTL
shHIF-1α
*
hCD10+CD19- B cell numbers
(among CD45+GFP+ cells)
shCTL
shHIF-1α
E
HIF-2α
[O2]↘
LMPP
T cell ↗
NK cell ↗
B cell ↗
Pro-T/NK
T cell ↗
NK cell ↗
HIF-1α
↗ Increase in comparison to normoxia
Functional effects of HIF-1/2α
Molecular effects of HIF-1/2α

Figure 7

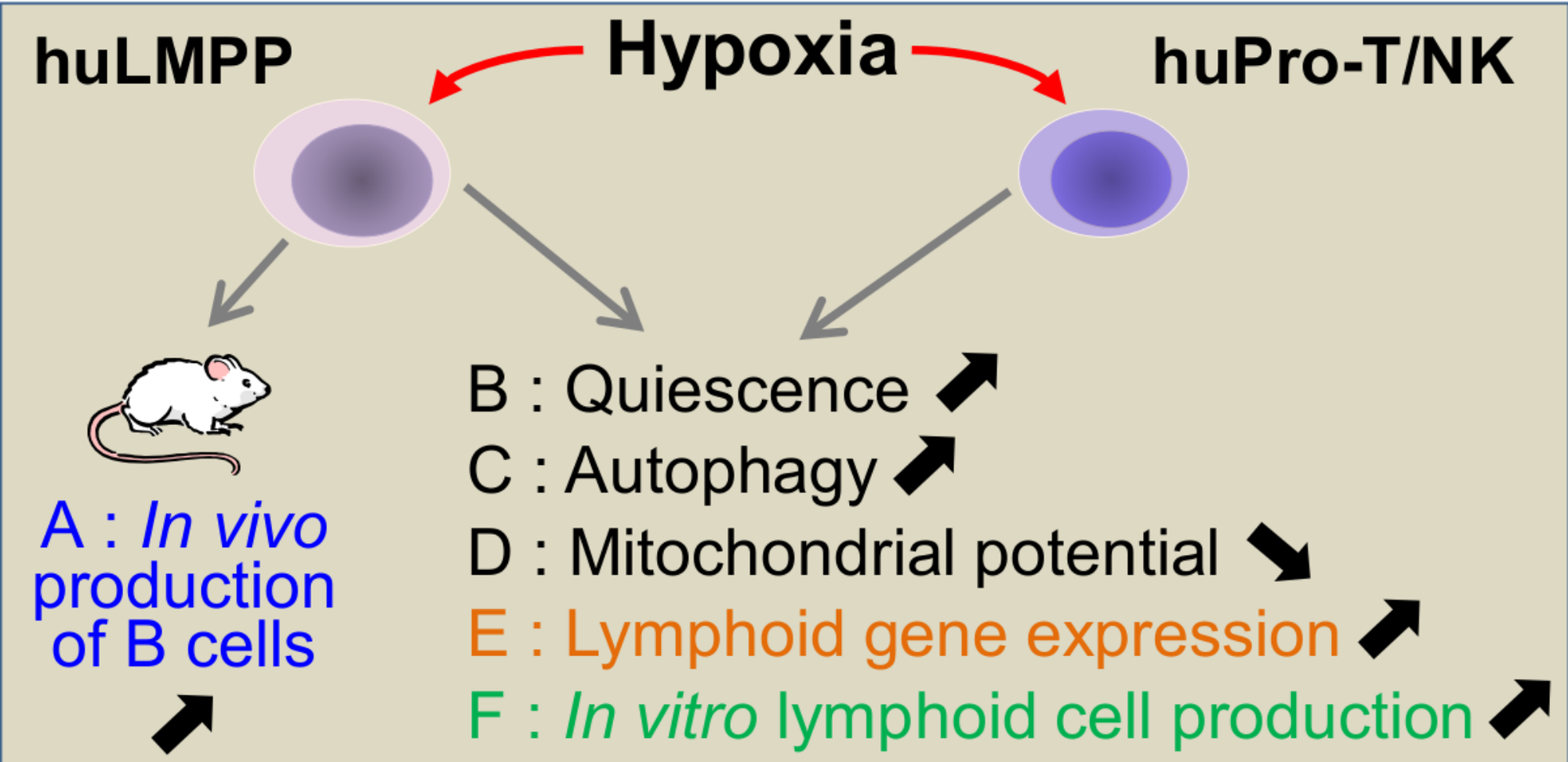

		huLMPP	huPro-T/NK
~~HIF-1α~~	A	↘	nd
	E	↘	↔ or ↗
	F	↔	↔
~~HIF-2α~~	E	nd	↘
	F	↘	↘